UNIVERSIDAD POLITECNICA DE VALENCIA

ESCUELA POLITECNICA SUPERIOR DE GANDIA

Master en Ingeniería Acústica

"Study of acoustic signals for the neutrino detector AMADEUS-ANTARES"

TESIS DE MASTER

Autor:
María Saldaña Coscollar

Director/es:
D. Miguel Ardid Ramírez
D. Joan Martínez Mora

GANDIA, 2011

Study of acoustic signals for the neutrino detector AMADEUS-ANTARES

Autor: María Saldaña Coscollar
Director1: Miguel Ardid Ramírez
Director2: Joan Martínez Mora

Resumen — En este se proyecto estudia aspectos acústicos pertenecientes al proyecto europeo ANTARES. Por una parte, se centra en el análisis de las señales acústicas recibidas en el sistema de posicionamiento AMADEUS-ANTARES. El programa desarrollado analiza las señales captadas por los sensores, las analiza de manera individual, aplicando una serie de filtros y transformaciones, extrayendo, la frecuencia, fase y amplitud propia de la señal. A continuación, se calcula el tiempo de subida y de bajada apropiado para la amplitud de la señal, con el que se obtiene su duración. La aplicación ha sido diseñada con objetivo de automatizar la detección y análisis de las señales recibidas del sistema, consiguiendo mayor precisión en la reconstrucción del posicionamiento de fuentes.
Por otra parte, se lleva a cabo el diseño y calibración de un array lineal de ocho hidrófonos que genera, de manera artificial, el pulso acústico bipolar generado por el neutrino de energía ultra alta en su interacción con el agua. El objetivo del array es transmitir al detector acústico de ANTARES la señal bipolar con similares características en amplitud, forma y directividad a la señal acústica creada por el neutrino en el agua. La calibración ha sido desarrollada combinando métodos de procesado de señal junto con medidas experimentales. El array de hidrófonos es posicionado coherentemente en fase, a distancias conocidas. Aplicado el retraso correspondiente, la señal acústica bipolar es obtenida con mayor amplitud y directividad. La simulación del array acústico es estudiada con el objetivo de conocer la longitud y diseño idóneo para la correcta transmisión de la señal bipolar hasta el detector.

Abstract — This academic work study acoustic aspects of the ANTARES detector European project. In one hand, the signal analysis processing for the acoustic signals received by the AMADEUS-ANTARES system. The software developed analyses the received signal of each sensor, applying specific filters and transformations in the frequency and time domain, getting the phase, frequency and amplitude of the signal. For the next step, it fixes the Rise Time and Fall Time appropriated for the signal and the signal duration is obtained. The application is developed for automating the detection and analysis of the received signals from the positioning system, achieving a higher accuracy.
On the other hand, an eight lineal array hydrophone is designed and calibrated for generate the artificial Ultra High Energy (UHE) neutrino-induced pulses. The array goal is the transmission of the bipolar acoustic signal pulse mimicking (simulating) the neutrino acoustic signal in terms of amplitude, shape and directivity to the ANTARES detector. The calibration is developed using signal processing methods within experimental measures. The array hydrophone is located coherently in phase with known distances. Hence, the delay between them is applied to get a higher amplitude and directivity acoustic bipolar pulse. The acoustic array simulation is studied in order to know the length and design for the proper bipolar signal transmission to the detector.

Autor: Maria Saldaña Coscollar, email: masalcos@epsg.upv.es
Fecha de entrega: 5-09-2011

INDEX

I. INTRODUCCIÓN

I.1 *PLANTEAMIENTO DEL PROBLEMA*

En esta tesina se desarrollan dos casos acústicos relacionados con el telescopio submarino de neutrinos implantado en el mar Mediterráneo, el detector ANTARES (Astronomy Neutrino Telescope and Abyss RESearch) [1]: el estudio de los datos acústicos recibidos en el sistema AMADEUS (Antares Modules for Acoustic DEtection Under the Sea) [2] para el sistema de posicionamiento, y por otra parte, la generación artificial del pulso acústico bipolar del neutrino en su interacción con el agua, mediante la calibración y diseño de un array lineal de hidrófonos.

I.2 *OBJETIVO Y ALCANCE DEL PROYECTO*

Los objetivos concretos del proyecto son los siguientes:

- Análisis y estudio de señales acústicas recogidas por el sistema AMADEUS, desarrollando, una aplicación de procesado de la señal con el fin de mejorar la detección de señales acústicas del sistema de posicionamiento y mejorar su precisión y exactitud, así como, la búsqueda de posibles fuentes acústicas puntuales que puedan afectar en la detección del sistema de posicionamiento.
- Calibración de un array lineal acústico compuesto por ocho hidrófonos encargado de generar artificialmente el pulso bipolar generado por el neutrino en su interacción con el mar. Alcanzando mayor precisión en la transmisión de datos debajo del agua, con el preciso control de amplitud y fase de la señal, siendo útil para la detección y calibración en el sistema AMADEUS-ANTARES.

Estos estudios son llevados a cabo con el fin de comprobar y mejorar el estado de operación del sistema AMADEUS perteneciente al detector submarino de neutrinos ANTARES.

I.3 *CONTEXTO DE LA INVESTIGACIÓN*

Por una parte, para el análisis de las señales acústicas captadas por el sistema AMADEUS, ha sido necesario el estudio del procesado de señales acústicas y análisis de datos, por lo que, documentación [3], software y aplicaciones informáticas han sido requeridos. Principalmente, se ha utilizado el software matemático computacional Matlab (MathWorks) para el desarrollo del programa de análisis. Todo el material necesario en su desarrollo ha sido otorgado por el personal e instalaciones del *Departamento de Física Aplicada* (DFA) en colaboración con el Instituto de Investigación para la Gestión Integrada de

zonas Costeras (IGIC) de la Escuela Politécnica Superior de Gandía (EPSG), Universidad Politécnica de Valencia (UPV).

Por otra parte, para la calibración del array acústico ha sido necesario el estudio de software y herramientas de procesado de señal para sistemas de simulación y generación de señales acústicas en el agua, e identificación de sistemas, utilizando para ello el software Maltlab (MathWorks) y LAbVIEW (National Instruments). Así como, en la utilización de la instrumentación, dispositivos y equipamiento utilizados en el desarrollo experimental en el tanque de agua del laboratorio.Este trabajo se ha llevado a cabo en el Departamento de investigación *Research School of Computing, Engineering and Information Sciences* (CEIS) perteneciente a Northumbria University (Newcastle, UK). Northumbria University participa en la colaboración ACorNE (Acoustic Cosmic Ray Neutrino Experiment) [4,5].

I. INTRODUCTION

I.1 *BACKGROUND*

This thesis develops the researching of two acoustic aspects from the neutrino submarine telescope installed in the Mediterranean Sea, the ANTARES (Astronomy Neutrino Telescope and Abyss RESearch) [1] detector where the AMADEUS (ANTARES Modules for the Acoustic Detection Under the Sea) [2] system is integrated: the study of the acoustic data received in the AMADEUS system for the positioning system, and on the other hand, the generation of the artificial Ultra High Energy (UHE) neutrino-induced pulse using an eight lineal array hydrophone.

I.2 *OBJECTIVES*

The specific goals of the project are:

- To study and analysis of the acoustic signal taken by the AMADEUS system, developing a signal processing application. To the purpose of improving the acoustic signals detection for the positioning system in accuracy and precision, as well as the seeking of acoustic sources which could affect on the detection for the positioning system.

- To calibrate an acoustic array of eight hydrophones which generates artificially the neutrino-induced bipolar pulse, achieving higher transmission data accuracy underwater, using the precise control of the amplitude and phase of the signal, being useful for the AMADEUS-ANTARES system calibration and detection.

This research has been done to check, test and improve the AMADEUS system operation state, belonged to the ANTARES neutrino submarine detector.

I.3 *RESEARCHING ENVIRONMENT*

On the one hand, for the acoustic analysis of the data recorded by the AMADEUS system, the study of acoustic analysis processing has been needed as theoretical information [3] as software and informatics application. Mainly, the Matlab (MathWorks) mathematical software has been used for the development of the analysis program.The needed material during the work progress has been given by the staff and installations of the *'Departamento de Fisica Aplicada* '(DFA) in collaboration with the 'Instituto de Investigación para la Gestion de Zonas Costeras' (IGIC) and the 'Escuela Politécnica Superior de Gandía' (EPSG), of the 'Universidad Politécnica de Valencia' (Valencia, Spain).

On the other hand, for the acoustic array calibration has been needed the study of signal processing analysis software and features for the underwater acoustic signal generation and simulation, using the Matlab software and LabVIEW(National Instruments), as well as, for the instrumentation, devices and equipment used has been required during the experimental measures on the water tank laboratory. This research has been developed on the *Research School of Computing, Engineering and Information Sciences* (CEIS) of the Northumbria University (Newcastle,UK). Northumbria University is the member of Acoustic Cosmic Ray Neutrino Experiment (ACoRNE) collaboration [4,5].

II. INTRODUCTION TO THE UNDERWATER NEUTRINO TELESCOPES

II.1. *UHE NEUTRINO DETECTION*

II.1.1 *Neutrino interest*

The interest for the observation and detection of very high energy (10 GeV-10 PeV) neutrinos has grown in recent years in order to study astrophysical objects of the Universe such as Active Galactic Nuclei, Gamma Ray Burst, Supernova remnant, or Dark Matter [6]. It could be very helpful as well in particle physics since it will allow testing astrophysical models through the neutrino interaction cross-sections or by comparing hadronic and electromagnetic processes. To obtain a good and complete description of the Universe it would be certainly interesting to observe and understand the internal composition of the

astrophysical object, to have observations and measurements in a large energy range and have the possibility of detecting particles from distant sources. All these aspects would be possible if there would be a messenger, which was easily produced in astrophysical sources, with no electrical charge, so it would not be affected by magnetic fields, and with small probability of interaction with the matter, so they can escape of dense media and travel long distances.

Neutrino belongs to a family of particles called “Leptons” (from the Greek word *leptos* meaning small or fine). Leptons exist in three flavours and each forms a couplet of one charged and one neutral particle as shown in the below figure:

e^-	μ^-	τ^-	$q = e$
ν_e	ν_μ	ν_τ	$q = 0$

Figure 1. The three doublet family charged and neutral leptons

Neutrino is An elementary fermion particle without electric charge. There are three kinds of neutrinos: electron neutrino (Ve), muon neutrino (Vu) and tau neutrino (Vt). And it has a very little mass but it is not zero. Specific properties of the neutrino particle make it very interesting to do astrophysics. As it has been pointed before, the interaction probability of the neutrino with the matter is very small, meaning that it will not be affected in its trajectory through the Cosmos to the Earth. It can, as well, escape from dense media allowing us to study the inner working mechanism of astrophysical objects. In addition, it is a neutral particle so magnetic fields do not affect the path along its Universe. On the other hand, the low probability of interaction makes difficult to detect them, and therefore, it is essential that neutrino telescopes have necessarily big volume detection, especially for the case of energetic neutrinos where the fluxes are not so high.

Neutrino detection is based on the measurement of the Cherenkov light induced by secondary leptons like muon produced by neutrino interactions with matter while passing across the Earth (Fig. (2)). Searches for cosmic ray neutrinos are ongoing in AMANDA [7], IceCube [8], ANTARES [1], NESTOR [9], NEMO [10], KM3NeT [11] and at Lake Baikal [12] detecting upward going muons from the Cherenkov light in either ice or water. In general, the muons detection from the Cherenkov light in either ice or water is sensitive to lower energies than discussed here since the Earth becomes opaque to neutrinos at very high energies. The experiments could detect almost horizontal higher energy neutrinos but have limited target volume due to the attenuation of the light signal in the media. Also, there are ongoing experiments to detect the neutrino interactions by either radio or acoustic emissions from the resulting particle showers because of the neutrino interaction in liquids [2, 13, 14]. These techniques, with

much longer attenuation lengths, allow very large target volumes utilising either large ice fields or dry salt domes for radio or ice fields and the oceans for the acoustic detection.

II.1.2. *Underwater neutrino telescope*

The main goal of underwater neutrino telescopes is the observation of astrophysical objects like Active Galactic Nuclei (AGN), Gamma Ray Bursts (GRBs), Microquasars, or Supernova Remnants. In fact, astrophysical objects that are able to accelerate protons and nuclei in a wide range of energy are possible candidates to be considered as neutrino sources due to a possible interaction of these accelerated cosmic rays with matter or radiation located in the surroundings of the source. Other interesting applications of underwater neutrino telescopes will be the indirect detection of dark matter using neutrinos generated by the annihilation of weakly interacting massive particles (WIMPs) captured by celestial bodies like the Earth, the Sun or even the Galactic Center. Finally, these detectors are also good for the understanding of some particle physics processes involving for example neutrino oscillations or neutrino interaction cross-sections. In addition, and due to the particular location of underwater neutrino telescopes, these infrastructures offer the possibility to extend the scientific program beyond the astroparticle physics field by including in the facility different sensors for Earth and Sea studies. The continuous monitoring of these sensors in real time is a powerful tool for environmental studies, and to bring some light in the understanding of different multidisciplinary problems such as ocean dynamics, climate change, etc.

Among the different kinds of neutrino interactions, the muon channel is the most suitable for astroparticle observation and the orientation and depth of the optical modules are selected to optimise the performance of this detection channel. Both, ice and water, neutrino telescopes have been designed taking advantage of the Earth as a shield, which stops all particles except neutrinos (very high energy neutrinos can also be stopped by the Earth). For this reason, we have to be able to detect upward-going muons that come from interactions and discriminate them from downward atmospheric muons. To reduce the huge amount of atmospheric muon background it is necessary that the neutrino telescope is installed in a deep site.

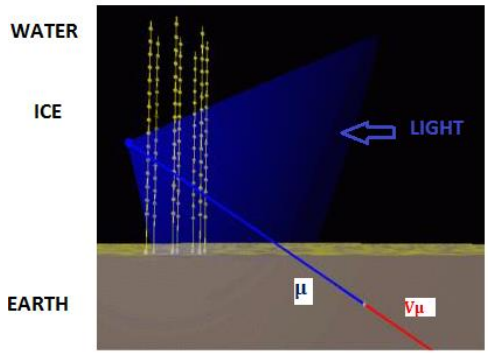

Figure 2. Neutrino interaction and detection scheme.

II.1.3. *Deep-Sea Acoustic Neutrino Detection*

In order to test the feasibility of detecting such neutrinos by the acoustic technique it is necessary to understand the production, propagation and detection of the acoustic signal from the shower induced by an neutrino interaction in a medium, incorporing the true attenuation of the sound which has been found to be complex in nature in media such as sea water. Such complex attenuation causes dispersion of the acoustic signal and complicates both the propagation of the sound through the water and the signal shape at the detectors. This aspects has been explained in a previuos publication [14].

II.1.4. *The Thermo-Acoustic model*

Measuring acoustic pressure pulses in huge underwater acoustic arrays is a promising approach for the detection of cosmic neutrino with energies exceeding 100 PeV. The pressure signals are produced by the particle cascades that evolve when neutrinos interact with nuclei in water. The resulting energy deposition in a cylindrical volume of a few centimetres in radius and several metres in length (from 5m to 10 m) lead a local heating of the medium which is instantaneous with respect to the acoustic process. This temperature change induces an expansion or contraction of the medium depending on its volume expansion coefficient. According to the thermo acoustic model, the accelerated motion of the heated volume a micro-explosion forms a pressure pulse of bipolar shape which propagates in the surrounding medium.

Coherent superposition of the elementary sound waves, produced over the volume of the energy deposition, leads to propagation within a flat disk-like volume called *pancake* in the direction perpendicular to the axis of the particle cascade; the total acoustic radiation is confined to a narrow angle which is less than 1º,it is a very directive *pancake* and short bipolar pulse.After propagating several hundreds of metres in sea water, the pulse has a characteristic frequency. Earlier studies predicted a pulse of around 10 kHz, whereas more recent studies predict a higher frequency of c. 23 kHz. As a reference example, shown in Fig.3, at 1 km distance in direction perpendicular to a ultra high neutrino energy (energy > 1 EeV, where 1 EeV= 10^{18} eV).

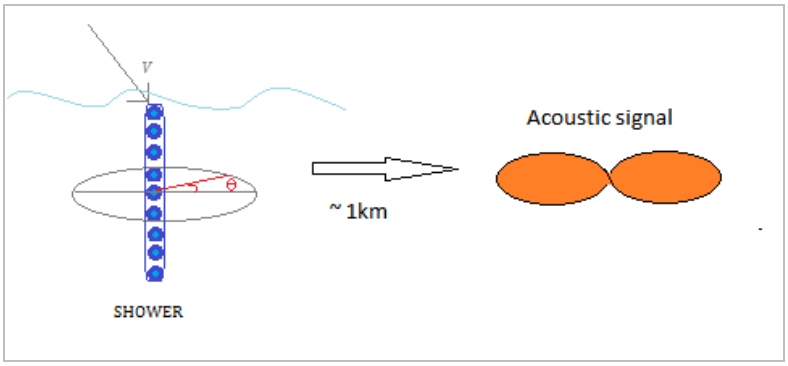

Figure 3. Scheme of the neutrino energy deposition in the water and the subsequent generation and propagation of the bipolar pulse

The production of pressure waves by fast particles passing through liquids was predicted as early as 1957 [15], leading to the development of the so-called thermo-acoustic model in the 1970s. According to the model, the energy deposition of charged particles traversing liquids leads to a local heating of the medium which can be regarded as instantaneous with respect to the typical time scale of the acoustic signals. Because of the temperature change the medium expands or contracts according to its volume expansion coefficient α. The accelerated motion of the heated medium produces a pressure pulse which propagates through the medium. The wave equation describing the pulse is:

$$\vec{\nabla}^2 p(\vec{r},t) - \frac{1}{c_s^2}\cdot\frac{\partial^2 p(\vec{r},t)}{\partial t^2} = -\frac{\alpha}{C_p}\cdot\frac{\partial^2 \varepsilon(\vec{r},t)}{\partial t^2} \qquad (1)$$

Here $p(\vec{r},t)$ denotes the pressure at a given place and time, c_s the speed of sound in the medium, C_p its specific heat capacity, α the thermal expansion coefficient and $\varepsilon(\vec{r},t)$ the energy deposition density of the particles.

The spatial and temporal distribution of $\in$ is not accessible to laboratory experiments at the relevant primary neutrino energies $E \approx 10^{18}$ eV and hence is subject to uncertainties. Simulations depend on both the extrapolation of parameterisations for lower energies into this regime and on the transcription of simulations for extended air showers to showers in water. Monte Carlo simulation of neutrino interactions in water for a cascade energy has been developed in previous studies [14,16], where the energy deposition is modelled using Monte Carlo points with a density proportional to energy, the pressure will be a scaled derivative histogram of the flight times to the observer. A further simplification can be made if the energy deposition as a function of time is identical at all points in the volume. If the observer is considered, for example, at a distance from the source along the X-axis much further away than the dimensions of the source, $p(t)$ can be defined by:

$$\begin{aligned} p(t-t_0) &= -\frac{\beta}{4\pi C_p}\frac{c}{x_0'-x'}\frac{d}{dt}E(c(t-t_0)) \\ &= \frac{\beta}{4\pi C_p}\frac{c^2}{x_0'-x}\frac{d}{dx'}E(x') \\ &\approx \frac{\beta}{4\pi C_p}\frac{c^2}{x_0}\frac{d}{dx'}E(x') \end{aligned} \qquad (2)$$

II.1.5. *Acoustic attenuation in the seawater*

The acoustic attenuation in seawater is almost totally caused by absorption. In the 1-100 kHz region it is dominated by a chemical relaxation process that is connected with the association-dissociation of magnesium sulphate ($MgSO_4$) ions under the pressure of the sound wave. Below 1 kHz a similar mechanism involving boric acid ($(B(OH)_3$) is responsible for much of the observed attenuation.

Taken together these mechanisms result in an attenuation of acoustic waves in seawater and a velocity of sound, which are both frequency dependent. Experimentally however whereas it is straightforward to estimate the magnitude of $|a|$ of the complex attenuation it is very difficult to determine the phase angle of a and no current measurements exist in the literature. The magnitude of the attenuation however is well measured and the definitive work in this area is considered to be that of Francois and Garrison [17]. More

recently, Ainslie and McColm [18] have published a simplified parameterization of the magnitude of the attenuation in seawater, which maintains a similar accuracy to the parameterizations of Francois and Garrison. This is a function not only of frequency but also depends on depth, *z*, salinity, S, temperature, T and pH. Whereas there are no direct measurements of the attenuation angle, Lieberman [19] gives a clear presentation of the chemical processes causing the attenuation while Niess and Bertin [20] have published a complex attenuation formula based on Mediterranean conditions. The ACORNE attenuation method [14] presents a complex version of the Ainslie and McColm formulation, which retains the attenuation magnitude but introduces the phase shifts predicted by Lieberman. In essence the attenuation consists of three components, two of these are complex, high pass filters with cut off frequencies ω_B (~$2\pi \times 10^3$ rad s^{-1}) for boric acid and ω_{Mg} (~$2\pi \times 10^5$ rad s^{-1}) for magnesium sulphate. The third is the pure water component, which is real. The ACORNE parameterization uses a_x values that are the respective attenuation coefficients in dB/km; boric acid (w_B), magnesium sulphate (w_{Mg}), boric acid and magnesium sulphate attenuation coefficients (a_B, a_{Mg}), water coefficient attenuation (a_w), and total attenuation coefficient ($a_{dB/km}$):

Boric Acid:

$$w_B = 1560\pi\sqrt{\frac{S}{35}}e^{T/26} \tag{3}$$

Magnesium sulphate:

$$w_{Mg} = 84000\pi e^{T/17} \tag{4}$$

Boric acid attenuation coefficient:

$$a_B = \frac{1.893\times10^{-4}}{2\pi}e^{\frac{pH-8}{0.56}} \qquad a_{Mg} = \frac{0.52\times10^{-3}}{2\pi}(1+\frac{T}{43})\frac{S}{35}e^{\frac{-z}{6}} \tag{5}$$

Water coefficient attenuation:

$$a_w = \frac{49\times10^{-9}}{4\pi^2}e^{-(T/27+z/17)} \tag{6}$$

Attenuation coefficient:

$$a_{dB/km} = \frac{a_B w_B s}{s+w_B} + \frac{a_{Mg} w_{Mg} s}{s+w_{Mg}} + a_w w^2 \tag{7}$$

where $s = i\omega$

The conditions in the Mediterranean Sea are in average are: T = 15ºC; S = 37; pH = 7:9. This new method of computing the acoustic signal complex attenuation for neutrino shower in water and ice has been described in collaboration with the ACORNE in the aricle mentioned previously [14]. The method allows the most up to date knowledge of the attenuation to be incorporated naturally, which is known to be complex in nature.

II.2. *ANTARES DETECTOR*

The ANTARES (Astronomy with a Neutrino Telescope and Abyss environmental RESearch) Collaboration has built a large effective area water Cherenkov detector in the deep Mediterranean Sea optimised for the detection of muons from high-energy astrophysical neutrinos. It is, at present, the largest neutrino telescope in the northern hemisphere and the largest underwater neutrino telescope in the world. This facility has represented a technological challenge since a large amount of sensors of different kinds had to be deployed and connected in deep sea to become a network of coordinated underwater sensors looking for neutrinos and monitoring the deep sea.

ANTARES telescope is located at a depth of 2475 m in the Mediterranean Sea (42º48′ N, 6º10′ E), 42 km from the French city of Toulon (France), Figure 1.4. To make this idea feasible a large European Collaboration (with more than 200 people among physicists, engineers and technicians from France, Germany, Italy, The Netherlands, Romania, Russia and Spain) has built, deployed an operated a detector with an effective surface area of about 0.1 km^2 composed of 12 vertical lines of about 450 m height and about 70 m spacing, holding 885 photomultipliers. Besides the optical module sensors, a set of calibration sensors, a data acquisition system and communication networks are needed. A specific dedicated instrumentation line with multidisciplinary oceanographic equipment and acoustic sensors have been deployed as well. All this configure a large interrelated network of systems of sensors looking for neutrinos and monitoring the deep sea.

ANTARES has the objective to detect and study very high-energy extraterrestrial neutrino sources, allowing us to open a new window to the Universe. Results from the telescope could produce a valuable insight not only in astronomy and astrophysics, but in particle physics, dark matter and cosmology as well. In addition, ANTARES houses instrumentation from other sciences like marine biology and geophysics for long term and on-line monitoring of the deep sea environment.

II.2.1. *ANTARES Design*

The ANTARES detector comprises 12 vertical structures, the *detection lines*. Each detection line holds up to 25 *storeys* that are arranged at equal distances of 14.5 m along the line, starting at about 100 m. They are all interlinked by electro-optical cables. A standard Storey consists of a titanium support structure, holding three *Optical Modules* (each one consisting of a photo multiplier tube (PMT) inside a water-tight pressure-resistant glass sphere) and one *Local Control Module (LCM).* The LCM consists of a cylindrical titanium container and the off-shore electronics within that container.

A 13th line, called *Instrumentation Line (IL),* is equipped with instruments for monitoring the environment. It holds six storeys. For two pairs of consecutive storeys in the IL, the vertical distance is increased to 80 m. Each line is fixed on the sea floor by an anchor equipped with electronics and held taut by an immersed buoy. An interlink cable connects each line to the *Junction Box* from where the main electro-optical cable provides the connection to the shore station.

The ANTARES lines are free to swing and twist in the undersea current. In order to determine the positions of the storey with a precision of about 20 cm—which is necessary to achieve the required pointing precision for neutrino astronomy—the detector is equipped with an acoustic positioning system [21]. The system employs an acoustic transceiver at the anchor of each line and four autonomous transponders positioned around the 13 lines. Along each detection line, five positioning hydrophones receive the signals emitted by the transceivers. By performing multiple time delay measurements and using these to triangulate the positions of the individual hydrophones, the line shapes can be reconstructed relative to the positions of the emitters. Currently, the sequence of positioning emissions is repeated every 2 minutes.

II.3.*THE ANTARES MODULES FOR ACOUSTIC DETECTION UNDER THE SEA (AMADEUS)*

The AMADEUS project was conceived to perform a feasibility study for a potential future large scale acoustic neutrino detector. For this purpose, a dedicated array of acoustic sensors was integrated into the ANTARES neutrino telescope. In the context of AMADEUS, the following aims are being pursued:

- Long-term background investigations (levels of ambient noise, spatial and temporal distributions of sources, rate of neutrino-like signals);
- Investigation of spatial correlations for transient signals and for persistent background on different length scales;
- Development and tests of data filter and reconstruction algorithms;
- Investigation of different types of acoustic sensors and sensing methods;
- Studies of hybrid (acoustic and optical) detection methods. In particular the knowledge of the rate and correlation length of neutrino like acoustic background events is a prerequisite for estimating the sensitivity of a future acoustic neutrino detector.

In particular the knowledge of the rate and correlation length of neutrino-like acoustic background events is a prerequisite for estimating the sensitivity of a future acoustic neutrino detector.Because the speed of sound is small compared to the speed of light, coincidence windows between two spatially separated sensors are correspondingly large. Furthermore, the signal amplitude is relatively small compared to the acoustic background in the sea, resulting in a high trigger rate at the level of individual sensors and making the implementation of efficient online data reduction techniques essential. To reduce the required processing time without sacrificing the advantages given by the large attenuation length, the concept of spatially separated clusters of acoustic sensors is used in AMADEUS. Online data filtering is then predominantly applied to the closely arranged sensors within a cluster.

II.3.1. *AMADEUS System Design*

AMADEUS is integrated into the ANTARES neutrino telescope in the form of *acoustic storeys* that are modified versions of standard ANTARES storeys, in which the Optical Modules are replaced by custom designed acoustic sensors. Dedicated electronics is used for the digitization and pre-processing of the analogue signals.

The AMADEUS system comprises a total of six acoustic storeys: three on the IL, which started data taking in December 2007, and three on the 12th detection line (Line 12), which was connected to shore in May 2008. AMADEUS is now fully operative and routinely taking data with 34 sensors. Two out of 36 hydrophones became in-operational during their deployment. In both cases, the defect was due to pressurization. The acoustic storeys on the IL are located at 180 m, 195 m, and 305 m above the sea floor. On Line 12, which is anchored at a horizontal distance of about 240 m from the IL, the acoustic storeys

are positioned at heights of 380 m, 395 m, and 410 m above the sea floor. With this setup, the maximum distance between two acoustic storeys is 340 m

AMADEUS hence covers three length scales: spacing of the order of 1m between sensors within a storey (i.e. an acoustic cluster); intermediate distances of 14.5 m between adjacent acoustic storeys within a line; and large scales from about 100 m vertical distance on the IL up to 340m between storeys on different lines. The sensors within a cluster allow for efficient triggering of transient signals and for direction reconstruction. The combination of the direction information from different acoustic storeys yields (after verifying the consistency of the signal arrival times at the respective storeys) the position of an acoustic source.

The AMADEUS system includes time synchronization and a continuously operating data acquisition setup and is in principle scalable to a large-volume detector.

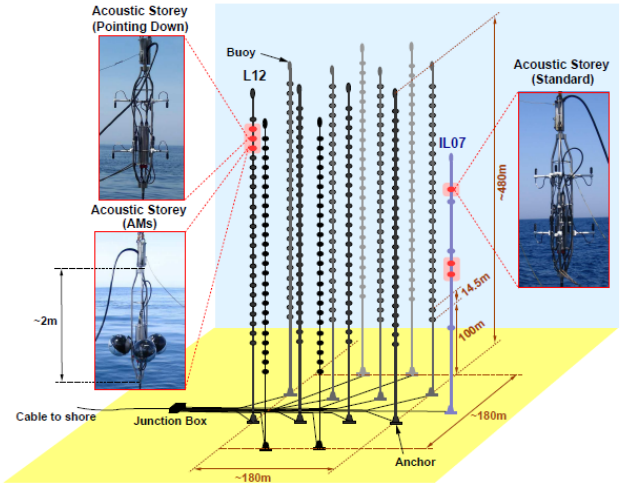

Figure 4 A sketch of the ANTARES detector. The six acoustic storeys are highlighted and their three different setups are shown (see text for details). L12 and IL denote the 12th detection line and the Instrumentation Line, respectively.

II.3.2. *AMADEUS Acoustic Storeys*

Two types of sensing devices are used in AMADEUS: hydrophones and Acoustic *Modules* (AMs). The sensing principle is in both cases based on the piezo-electric effect. For the hydrophones, the piezo-elements are coated in polyurethane, where as for the AMs they are glued to the inside of standard glass

spheres which are normally used for Optical Modules. The acoustic storeys on the IL house hydrophones only, where as the lower most acoustic Storey of Line 12 holds AMs. The hydrophones are mounted to point upwards, except for the central acoustic Storey of Line12, where they point downwards, an example is shown in the Fig.5. The sensitivity of the hydrophones is largely reduced at their cable junctions and therefore shows a strong dependence on the polar angle. The different configurations allow for investigating the anisotropy of ambient noise, which is expected to originate mainly from the sea surface. Three of the five storeys holding hydrophones are equipped with commercial models, dubbed "HTI hydrophones", and the other two with hydrophones, developed and produced at the Erlangen Centre for Astroparticle Physics (ECAP).

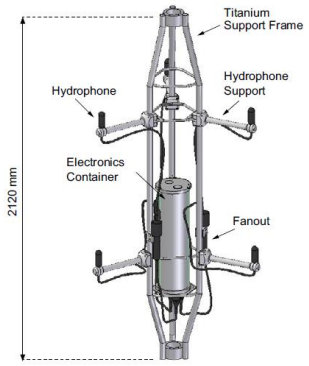

Figure 5. Drawing of a standard acoustic storey (acoustic cluster), with hydrophones.

(a) (b) (c)

Figure 6. Photographs of three different storeys of the AMADEUS system during their deployment: (a) A standard storey, equipped with hydrophones pointing up; (b) the central acoustic storey on Line 12 with the hydrophones pointing down; (c) the lowermost acoustic storey on Line 12 equipped with Acoustic Modules.

Three of the five storeys holding hydrophones are equipped with commercial hydrophones 2 and the other two with hydrophones developed and produced at the Erlangen Centre for Astroparticle Physics (ECAP). All acoustic sensors are tuned to be sensitive over the whole frequency range of interest from 1 to 50 kHz with a typical sensitivity around −145 dB ref 1V/μPa (including preamplifier) and to have a low noise level [22]. The sensitivity of a typical hydrophone is shown in Fig.7 as a function of frequency and the azimuthal angle [23].

The equivalent inherent noise level in the frequency range from 1 to 50 kHz is about 5.4 mPa for the AMADEUS hydrophones with the smallest such noise. This compares to 6.2 mPa of the lowest expected ambient noise level in the same frequency band for a completely calm sea [24], referred to as *sea state 0* [25].

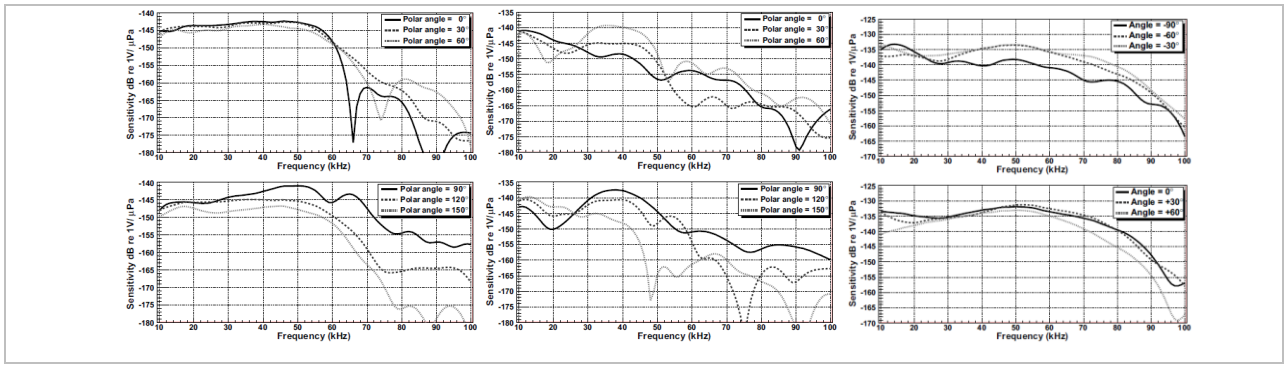

a) b) c)

Fig 7. Typical sensitivity as a function of frequency for different polar angles, averaged over the azimuthal angle. Systematic uncertainties below 50 kHz are 2 to 3 dB; a) HTI hydrophone b) ECAP hydrophone c) AM sensor.

Bipolar signals selected with the pulse shape recognition trigger typically have a signal-to-noise ratio exceeding 2 for a single sensor. Assuming a noise level of 10 mPa in the frequency range from 1 to 50 kHz, which is a typical level recorded at calm sea, i.e. sea state 0, a signal of 20 mPa can be detected.

II.3.3. *On- Shore Data Processing*

An on-shore computer cluster is used to process and filter the data stream and store the selected events. The system is operating continuously and automatically, requiring only little human intervention. It currently consists of four server-class computers, of which two with a total of 12 cores are used for data

triggering. One of the remaining two computers is used to write the data to an internal 550 GB disk array, while the other is used to operate the software for the online control of the data acquisition and other miscellaneous processes and to provide remote access to the system via ~~the~~ Internet. The AMADEUS trigger searches the data by an adjustable software filter; the events thus selected are stored to disk. This way the raw data rate of about 1.5 TB/day is reduced to about 10 GB/day for storage. Currently, three trigger schemes are in operation [2, 26]: A minimum bias trigger which records data continuously for about 10 s every 60 min, a threshold trigger which is activated when the signal exceeds predefined amplitude, and a pulse shape recognition trigger. For the latter, a cross-correlation of the signal with a predefined bipolar signal, as expected for a neutrino-induced cascade, is performed. The trigger condition is met if the output of the cross-correlation operation exceeds a predefined threshold. With respect to a matched filter, this implementation reduces the run time complexity while yielding a comparable trigger performance. In total, 1.6 TB of data were recorded in 2008 and 3.2 TB in 2009.

II.3.4. *The Acoustic Positioning System*

The Acoustic Positioning System (APS) is composed by a set of transceiver hydrophones located at the bottom of each line, some autonomous transponders on the sea floor and five receiver hydrophones located at storeys 1, 8, 14, 22 and 25, to monitor some strategic points of the line and minimise the uncertainties in the shape reconstruction since the positions of these receiver hydrophones are the data input used in the mechanical model fits. Electronic boards manage the settings of the system, for emission, reception, 35 detection, filtering and communication. The emitters generate a tone burst signal of 2 ms in a specific frequency of the [40 kHz – 60 kHz] frequency range [21]. This frequency range is justified, in one hand, because it has an optimal spatial resolution and, on the other hand, by having an acceptable attenuation length at the distances of hundreds of meters. Measurements for the line shape reconstruction are performed every 2 minutes with the completion of an ‘acoustic run’. At the present time each acoustic run consists of fourteen cycles; each individual cycle being associated with the emission of an acoustic signal from a single acoustic emitter. For each cycle, the signal transit time and the intensity level to the different receivers is recorded. Since the time of emission is known, the sound travel time between emitter and each receiver for all lines can be computed. Taking into account the profile of sound velocity obtained by different acoustic sound velocimeters and CTDs located along the detector and considering the sound travel time obtained previously, it is possible to calculate the distances between emitter and receivers. The excellent time resolution of the system of few μs, allows obtaining the distances between fixed transducers with stability better than 1 cm. Finally, the final positions of the receiver hydrophones are obtained by an algorithm based on triangulation method applied to the distances

between emitters and receivers calculated for the fourteen cycles. This is an important task for the achieving an accurate positioning of unknown sources, studies for the positioning system reconstruction has been done in previous works [27]. The Fig.8 shows the radial displacement of all hydrophones on Line 11 during a 16 week period.

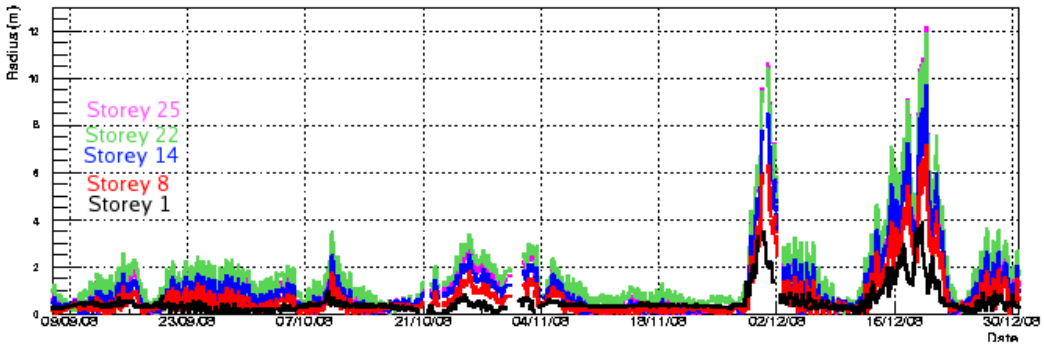

Figure 8: Radial displacement of line 11 over 16 week period time.

III. AMADEUS ACOUSTIC DATA ANALYSIS

III.1. *INTRODUCTION*

The precise determination of the relative positions of the Acoustic Storeys within ANTARES detector is a significant task of the AMADEUS system in order to provide an accurate positioning of unknown sources. Reconstruction methods have been analysed in previous studies [27]. The method used is to calculate the differences between the absolute time of signal emission and reception from several pingers to reconstruct the position of each hydrophone individually. The differences in arrival times of a pinger signal in the 6 hydrophones of a storey are used to reconstruct the direction of a pinger signal. Therefore, the adequate rise time and fall time determination for the reception signals at the hydrophones is an important measure to achieve precise signal detection, hence, the positioning reconstruction method can be improved in accuracy.

In this work, first studies are done in order to know the proper rise time and fall time determination. Signal processing is applied to analyse the signals received in the hydrophones for the system positioning.

III.2. *PROGRAMING ENVIRONMENT*

The processing, filtering and analysis of the acoustic data has been done using the software Matlab. This software provides functions really flexible and useful for the acoustic data managing.

III.3. *ANALYSIS EXECUTION*

III.3.1. *Data Signals*

The AMADEUS data under studied are the signals recorded from the transceivers (‘pingers’) of the ANTARES acoustic positioning system. The data from the acoustic run 33925 is analysed for this study and the final application is used with data from the acoustic run 33928 for comparison and validation of the system analyses. The acoustic run 33925 has recorded 17 fast cycles at well-defined frequencies within the range from 44522 to 60235 Hz by 6 sensors hold on the same Acoustic Storey. The signals are tone burst of 2 ms, this time duration means 500 samples for each signal, considering that the used frequency sample to register the data was 250 kHz. Each sensor has received the same tones emitted by ‘pingers’ from different lines (positions). In the Fig.9 in left panel (a) the cycle receptions in the Sensor number 6 is shown and in right panel (b) one of the single signal reception is shown.

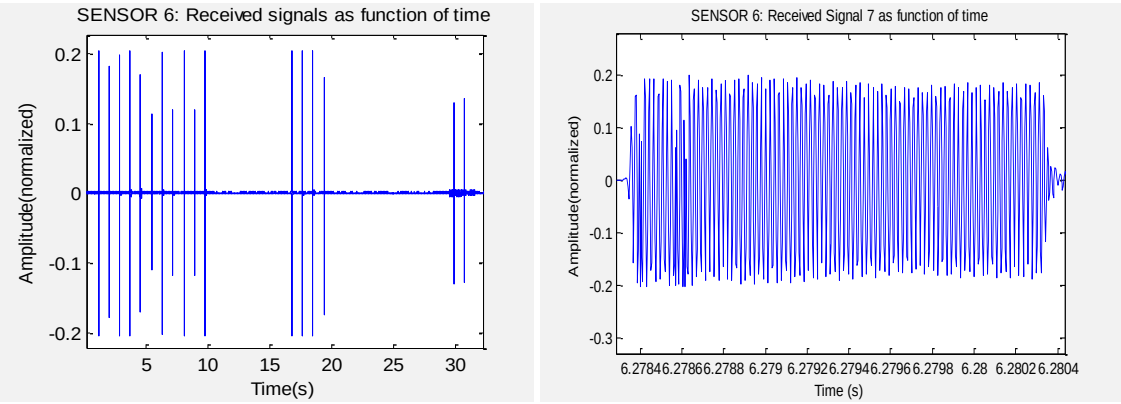

(a) (b)

Figure 9. (a) Received signals in the Sensor 6 at the storey. (b) Single received signal of Sensor 6.

III.3.2. *Results and analysis*

The final system application for the determination of the signal processing parameters method is set studying the received signals with less added noise, called 'clear' signal, in order to simplify it. For the sensors 6 to 9 the most 'clear' signals are the number 5 and 7. The final system application is realized after a previous study which contains these steps:

- Band Pass filtering and method
- Frequency margin of the Band Pass Filter
- Envelope method
- Proper % for the rise time (Tr) and fall time (Tf)

- Band Pass Filtering and method:

The first step is filtering the signals to avoid possible added noise from other frequency bands in order to get the interest signal under test. IIR filters are used for the Band Pass Filter study, although the FIR filters have a lineal phase and higher stability, a higher order is required, it means higher signal delay and computational cost (Figures). Hence, the comparison between a Tchebychev Filter and Butterworth Filter is realized, in order to know which one present the best relation between phase linearity level, amplitude and frequency response, as well as the required computational cost (Table 1). For this study, the wide frequency margin of 10 kHz is used.

COMPARISON FILTERS	**Rs=10 Rp=3**		**Rs=10 Rp=0.1**		**Rs=40 Rp=3**	
	Butter	Tcheby	Butter	Tcheby	Butterworth	Tcheby
Amplitude Response	***Very good***	***Bad***	***Good***	***Good***	***Very good***	***Very bad***
Phase Linearity	***Very good***	***Bad***	***Good***	***Bad***	***Bad***	***Very Bad***
Frequency response	***Very good***	***Bad***	***Good***	***Good***	***Very good***	***Very good***

Table 1. Amplitude response, Phase linearity and frequency response comparison between Butterworth and Tchebychev Pass Band Filter.

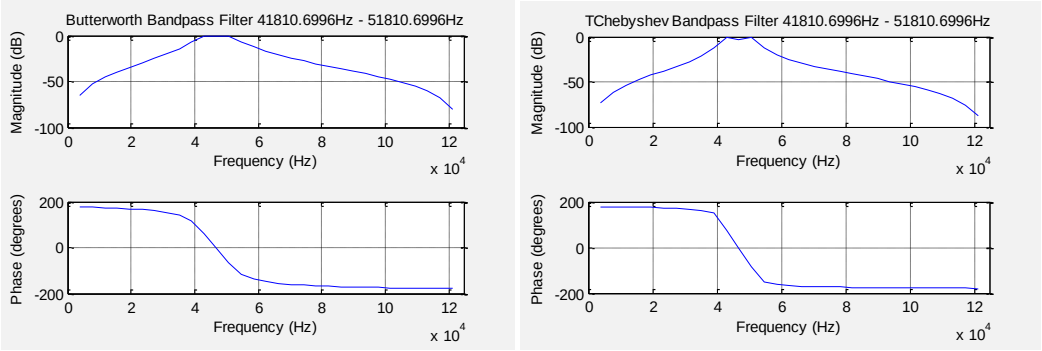

(a) (b)

Figure 10. Phase and Magnitude of Band Pass Filter for 10 kHz of frequency margin and Rstop= 10 and Rpass=3: (a) Butterworth filter, (b) TChebychev filter.

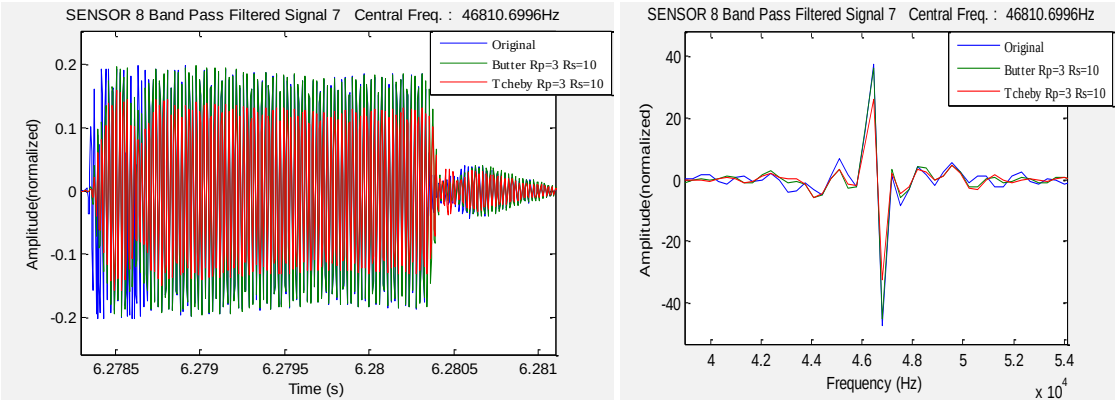

(a) (b)

Figure 11. Signal 7 from Sensor 8 filtered by Butterworth and Tchebychev Band Pass filters, for Rp= 3 and Rs= 10 using 10 kHz margin frequency: (a) Normalized amplitude vs time, (b) Zoom of normalized amplitude vs frequency.

- Frequency margin of the Band Pass Filter:

The frequency margin of the Band Pass Filter is studied for achieving a narrow Band Pass Filter which does not modify the original signal shape in terms of amplitude, phase and frequency.

The Butterworth Band Pass Filter is analysed for three different margins: 10, 5 and 2.5 kHz (Fig. 12).

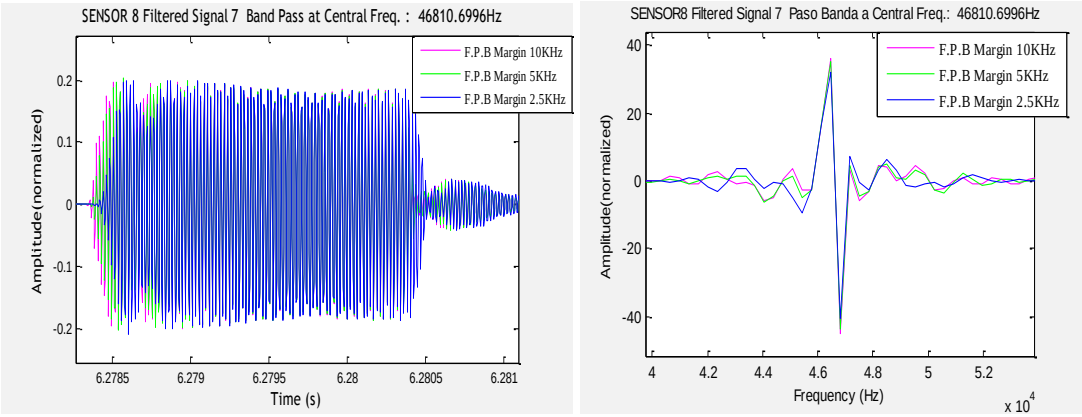

(a) (b)

Figure 12. Comparison between the Frequency margin: 10 kHz-5 kHz-2.5 k Hz, applying the Butterworth Band Pass Filter with Rp=3and Rs=10: (a) Normalized amplitude vs time;(b) Zoom of Normalized amplitude vs frequency;(c) Zoom of normalized amplitude vs frequency.

- Envelope method:

The envelope of the signal is equivalent to its outline and an envelope detector connects all the peaks in this signal. Envelope detection has numerous applications in the fields of signal processing and communications, one of which is amplitude modulation (AM) detection. The following block diagram (Fig.13) shows the implementation of the envelope detection using the two methods.

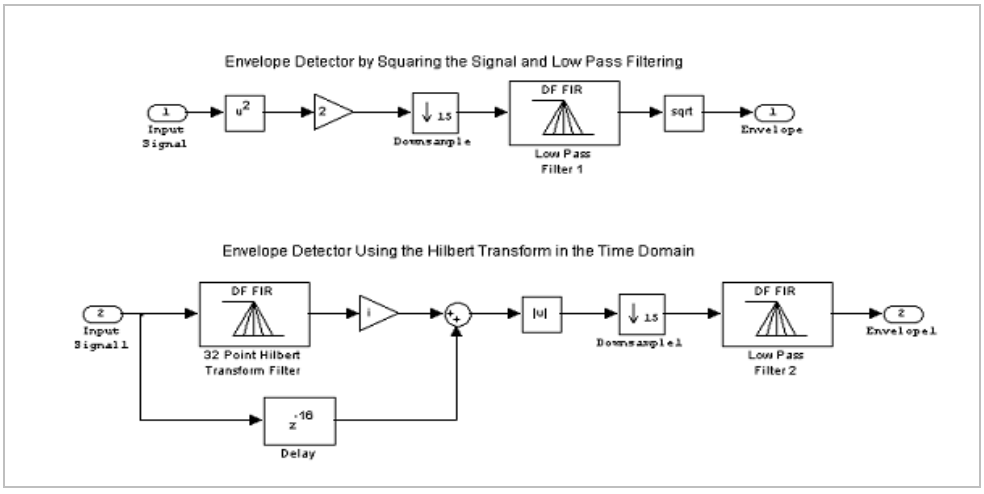

Figure 13. Block diagram of the envelope detection methods; the upper diagram shows the Squaring and Low Pass Filtering Method and the lower diagram shows the Hilbert Transform Method in the Time Domain.

The obtaining of an accurate amplitude detection tool is an important task for the signal analysis of the positioning system detection. The two methods described above are studied and compared (Fig. 14).

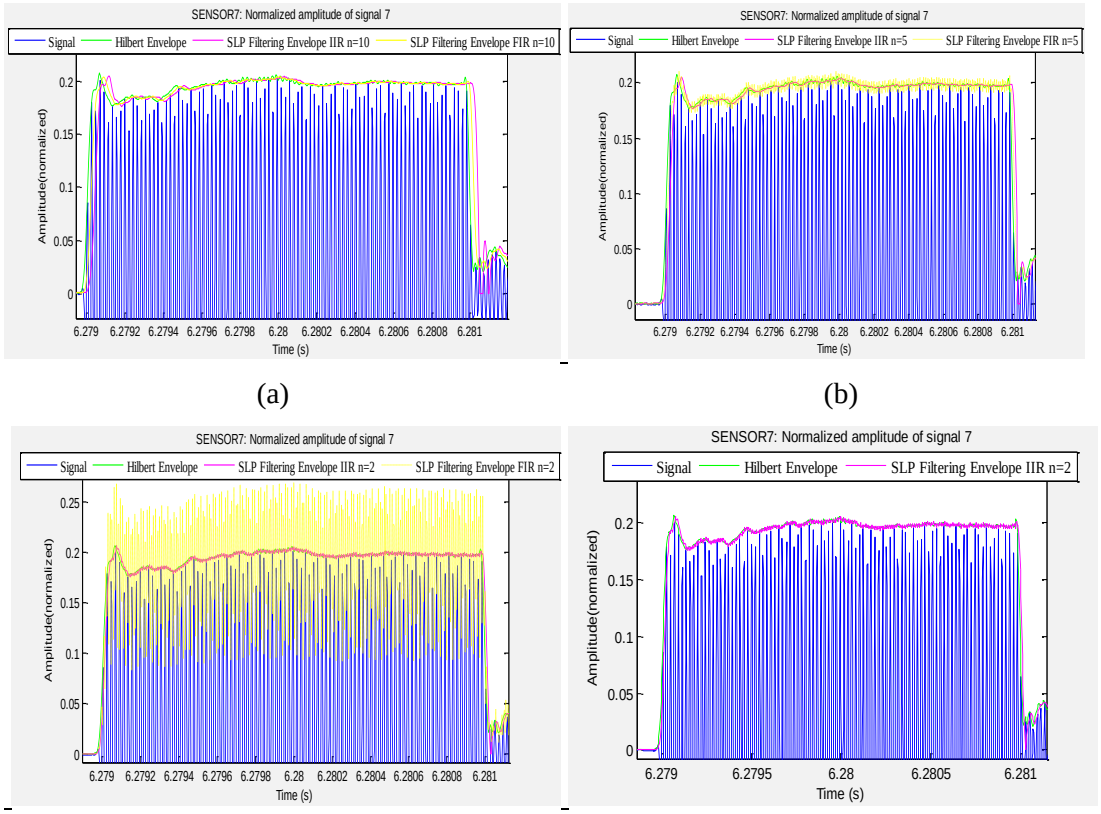

Figure 14. Zoom Envelope using Hilbert Method and Squaring-Low pass filtering Method (filter FIR and IIR): (a) Normalized amplitude vs time for order filter n= 10 ;(b) Normalized amplitude vs time for order filter n= 5; (c) Normalized amplitude vs time for order filter n=2. (d) Zoom Envelope using Hilbert Method and Squaring-Low pass filtering IIR of filter order=2, plotting the normalized amplitude vs time.

- Rise time and fall time:

Defining the rise time (Tr) as signal transition time from invalid low amplitude value to valid high amplitude value of the signal received, and the fall time (Tf) as signal transition time from high amplitude value to low amplitude value. These parameters are significant and necessaries for reliable measuring of burst detection and duration characterization. The accurate selection of Time rise (Tr) and Time fall (Tf) to obtain the most approximated signal duration is an important task in the signal detection. In order to achieve this objective, on the one hand, the comparison between 25, 50, 75 and 90 % of the signal amplitude has been done calculating the duration in samples for each Tr % and Tf % (the original signal has 500 samples duration). In this study has been selected the most 'clear' signals received with the Sensors 6 to 9, recorded in two different times, with a total of 11 signals analyzed. The statistical study has been done for measuring the samples average and the samples variability for the average measured, in the Table 2 is shown the results of the Sample Average (μ), the Standard Deviation (σ) and the Coefficient of variation(C_v). On the other hand, the same study is done just for the two most 'clear' signals received, shown in Table 3.

	Samples Average (μ)	Standard Deviation (σ)	Coefficient of variation (C_v)
Tr25% - Tf25%	520.00	20.63	0.0397
Tr25% - Tf50%	509.44	3.96	0.0078
Tr25% - Tf75%	505.90	3.65	0.0072
Tr25% - Tf90%	499.25	23.08	0.0462
Tr50% - Tf25%	516.38	20.76	0.0402
Tr50% - Tf50%	505.83	4.18	0.0083
Tr50% - Tf75%	502.29	3.81	0.0076
Tr50% - Tf90%	495.63	23.06	0.0465
Tr75% - Tf25%	512.57	20.97	0.0409
Tr75% - Tf50%	502.02	4.50	0.0090
Tr75% - Tf75%	498.48	4.19	0.0084
Tr75% - Tf90%	491.82	23.09	0.0470
Tr90% - Tf25%	508.25	22.97	0.0452
Tr90% - Tf50%	497.69	9.03	0.0181
Tr90% - Tf75%	494.15	8.84	0.0179
Tr90% - Tf90%	487.50	26.32	0.0540

Table 2. Average **(μ)**, Standard Deviation **(σ)** and Variation Coefficient (C_v) of the samples from 11 different 'clear' signals received by the Sensors 6, 7, 8 and 9.

	Samples Average (μ)	Standard Deviation (σ)	Coefficient of variation (C_v)
Tr25% - Tf25%	519.86	19.93	0.0383
Tr25% - Tf50%	508.00	5.50	0.0108
Tr25% - Tf75%	503.00	3.82	0.0076
Tr25% - Tf90%	467.86	77.21	0.1650
Tr50% - Tf25%	515.57	20.40	0.0396
Tr50% - Tf50%	503.71	5.92	0.0118
Tr50% - Tf75%	498.71	4.23	0.0085
Tr50% - Tf90%	463.57	76.71	0.1655
Tr75% - Tf25%	509.29	21.10	0.0414
Tr75% - Tf50%	497.43	6.86	0.0138
Tr75% - Tf75%	492.43	5.42	0.0110
Tr75% - Tf90%	457.29	75.84	0.1658
Tr90% - Tf25%	503.14	22.27	0.0443
Tr90% - Tf50%	491.29	8.65	0.0176
Tr90% - Tf75%	486.29	7.61	0.0157
Tr90% - Tf90%	451.14	75.13	0.1665

Table 3. Average **(μ)**, Standard Deviation **(σ)** and Variation Coefficient (C_v) of the samples from the 2 most 'clear' signals received by the Sensors 6, 7, 8 and 9.

III.3.3. *Analysis conclusion*

The conclusions of the complet signal received analysis are explained below:

- The Square and Low Pass Filtering method executed by a IIR Low Pass filter of high order (n=10) gives a softer envelope than being executed by a FIR filter, but a higher delay between the original signal and the envelope is obtained. Going down the Low Pass filter order (n= 5, 2) IIR filter improves the delay, obtaining better results in envelope and delay than using the FIR filter.

The comparison between Hilbert method and Square and Low Pass, using a low order IIR filter (n=2), show more accurate results using the Hilbert Method.

- The Butterworth Band Pass Filtering gets better amplitude and phase response than Chebychev filter, using the same Rpass and Rstop.

The comparison between the different Rpass and Rstop, shows the best approximation, with the original signal, in time, frequency, phase and amplitude response, using the Butterworth filter of Rpass= 3 and Rstop= 10.

- Comparing the Band Pass Filtering between the ranges of 10 kHz, 5 kHz y 2.5 kHz. A remarkable signal delay and amplitude is lost between the filtered signal and the original signal for the frequency range of 2.5 kHz. The 5 kHz and 10 kHz filtering give a slight and similar delay compared with the original signal, considering the 5 kHz filter narrower, it is chosen as a proper range frequency for the Band Pass Filter.
- The comparison between the different % rise Time and fall time shows the more accurate signal duration with the Time rise for 25% and 50 % with the same Time fall for 75% signal amplitude. The samples are more approximated to the original signal for the Time rise of 50 % amplitude but it has higher deviation. In order to resolve this point deeply the variation coefficient has been calculated, being lower for Tr= 25% and Tf= 75% signal amplitude. The two most 'clear' signals inside of the analysed signals show the same sample average approximation between them compared with the original signal, for Tr=25% and Tf=75% is obtained lower variability. Finally the Time rise for the 25% of the signal amplitude and the Time fall for the 75 % of the amplitude is chosen for the next reasons:

- The sample average is closed to the range of 500 samples.
- It has low dispersion.
- The times have the same symmetry; Tr goes up from 0 to 25% and Tf goes down from 100 to 75%.
- The noise normally is low, so Tr for 25% and Tf for 75% should be adequate.

The Fig.15 shows the diagram of Time Rise and Time Fall selected for the reception signal analysis.

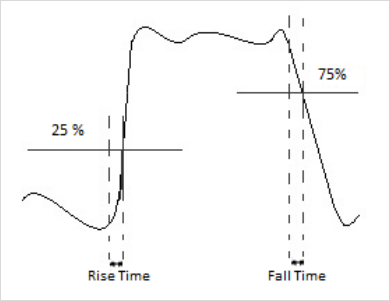

Figure 15. Diagram of Rise-Time and Fall-Time of the signal received analysis.

III.3.4. *Final system methodology*

The steps executed for the acoustic data processing application consist of:

1. To read acoustic signals received by one sensor .wav and extract the number of sample, sample rate and number of bits for the codification.
2. To create envelope of the received signals using 'The Hilbert Transform' and 'Squaring and Low Pass filtering' method. And detect each tone burst received (single burst tone) by the same sensor.

Then for each single tone received for the same sensor, the program follows the next commands:

1. To transform the single tone to frequency domain using the Fourier Transform, showing the frequency domain.
2. To apply a Band Pass Filter between the 35 kHz - 65 kHz frequency range.
3. To detect the central frequency of the single signal. Then, apply a narrower Band Pass Filter which has a 5 KHz range frequency.
4. To show the amplitude, phase and frequency vs time.
5. To transform the signal to time using the Inverse Fourier Transform.
6. To calculate the signal amplitude, obtaining the mean of the signal stable part amplitude.
7. To calculate the Time rise (Tr) and Time fall (Tf) of the signal, Tr for the 25 % of amplitude and Tf for the 75% of amplitude.
8. To obtain the duration of the signal.

III.3.5. *Study of problematic cases*

For this study the signals recorded for the sensors 6 to 11 (belonged to the same storey) recorded at the same period of time has been chosen. The most problematic received signals are the number 4, 11, 12, 13 and 14 within the sensors from 6 to 9, it is known observing the number of samples obtained, which is considerable higher or lower than 500 duration samples (the original signal duration), as well as observing the frequency and amplitude response which have high variability. The Fig.16 plots an example of the frequency components of the original received signal from 0- 100 kHz, the band pass filtered signal for 40 kHz to 60 kHz range and the pass band filtered signal with 5 kHz of margin, for the clear signals received 5 and 7 (Fig.16 (a) and (b)) and for the problematic signals received 11 and 12 (Fig.16 (c) and (d)), belonged to the sensor 6 for comparison. The problematic signals received show peaks at several punctual frequencies. These can be originated from the same source, showing all of the signals similar frequencies affections. In the Fig.17 the amplitude, the frequency and the phase vs time for the same signals are

plotted. The problematic signals amplitude (Fig.17 (c) and (d)) shows lower level in the points where the frequency is affected.

The possible causes of this effect in the problematic received signals could be the next ones:

- Signal clipping in the data acquisition module.

- Reflections, in the structure close to the acoustic sensor.

- External transient noise: bio noise and environmental.

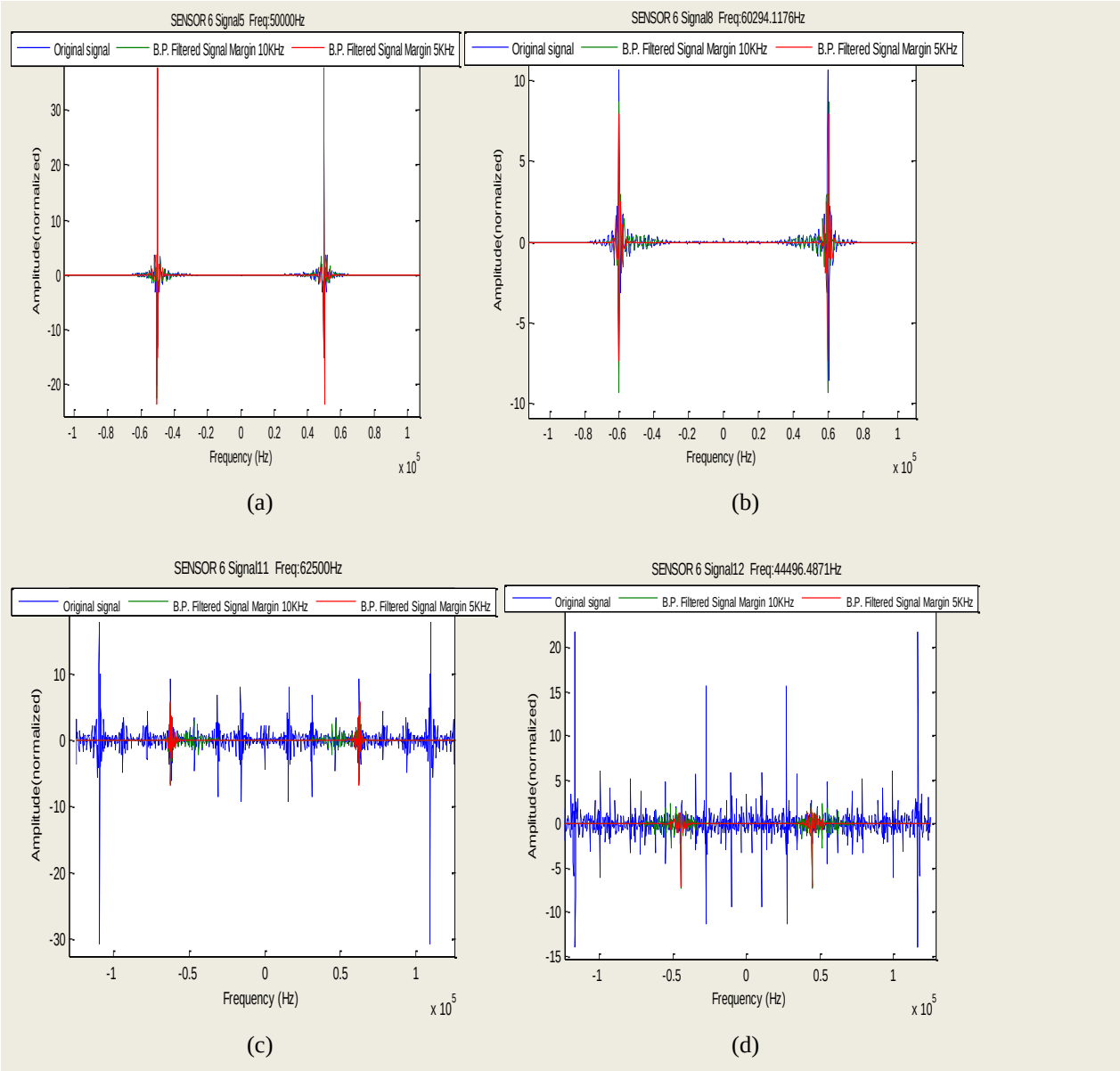

Figure 16. Frequency components (Fourier Transform) ; (a) 'Clear' signals received 5 and 7, (b) 'Problematic' signals received 11 and 12. All of them detected for the sensor 6.

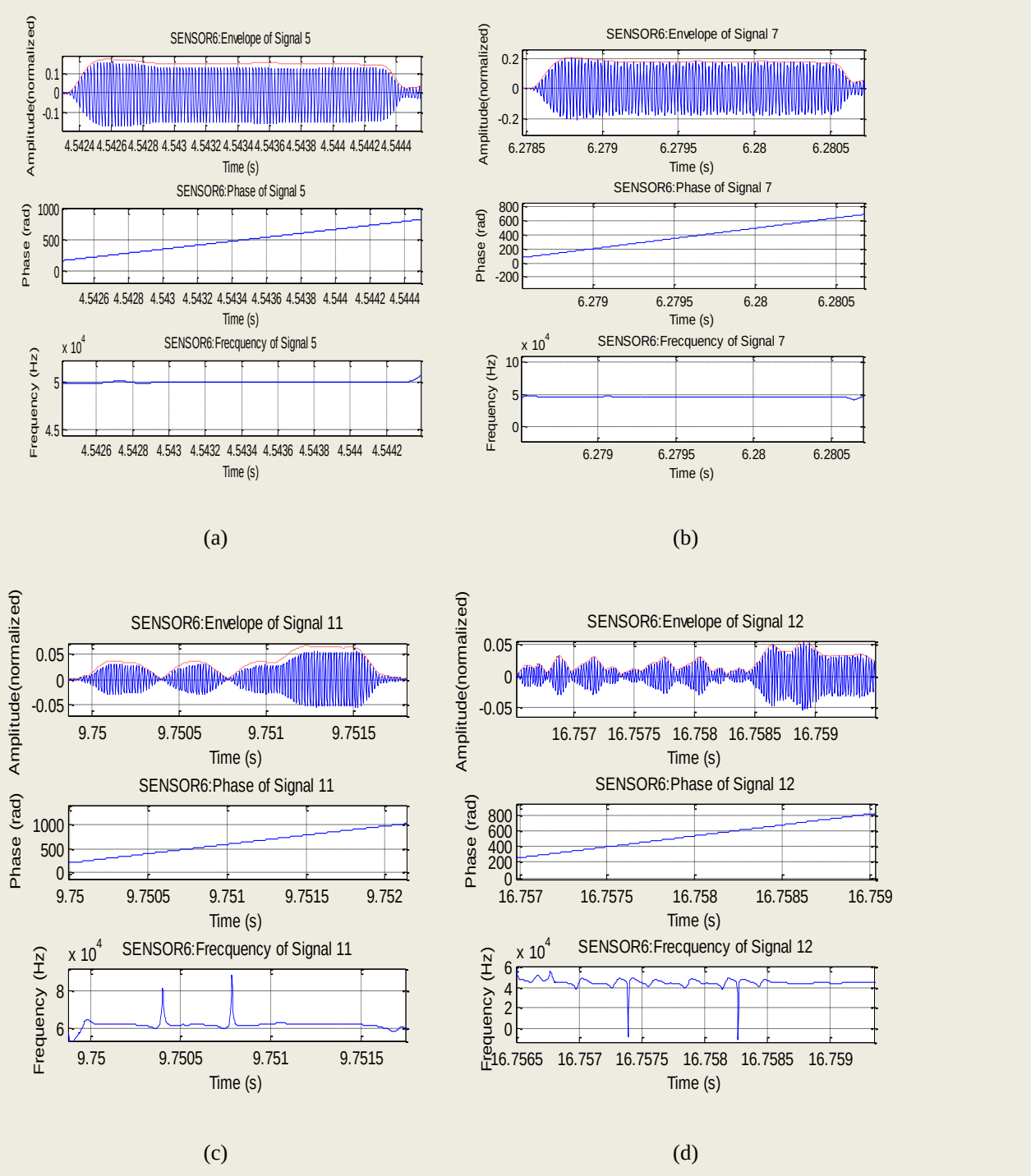

Figure 17. Amplitude, frequency and the phase vs time; (a) 'Clear' signals received 5 and 7, (b) 'Problematic' signals received 11 and 12. All of them detected for the sensor 6.

IV.4. *CONCLUSIONS*

The different analyses made and the results obtained permit to validate the correct running for the signal processing application to analyze the signals received for the positioning system detector at the AMADEUS system. This application allows obtaining accurate acoustic signal time and amplitude detection via signal processing. It can be considered as tool to improve the accuracy of the positioning system detection and as preliminary phase to realize a vast analysis from the received signal in order to study any possible external noise or behavior which could affect in the positioning detection.

In future job, the application can be use as a helpful tool to realize an accurate signal detection as well as to realize a deeper signal analysis of the received data from the positioning system, hence it can be extended in order to get more results and aspects from the signal and system detection which can be of interest in ANTARES or future neutrino telescopes, such a KM3Net.

IV. ACOUSTIC ARRAY CALIBRATION FOR GENERATION OF UHE NEUTRINOS

IV.1. *INTRODUCTION*

The evaluation of the acoustic neutrino detector behaviour in the field is a significant task under study. Hence, acoustic transmitters are needed to send artificial acoustic signatures from UHE neutrino interactions in the sea to the AMADEUS system. The transmitters have to be able to imitate the UHE neutrino acoustic pulse, in directivity (pancake) and shape (a short bipolar pulse). Furthermore the detector site is located at a depth of 2475 m underwater. Due these limitations, it is not an easy task to design a system able to transmit an acoustic bipolar pulse with such characteristics. The deployment and operation in site have to be considered in terms on the system design as well. The development of a compact transmitter using the parametric acoustic source technique has been studied to achieve the objective [28]. Previous studies in the calibration of single hydrophones for the UHE neutrino emulation were presented [29]. However, a single hydrophone only gives knowledge of the signal shape and the radiation is essentially omni-directional. In reality the pulse from a neutrino interaction should be highly direction.

This can be emulated using a line array. In addition because of the coherent nature of detection, the energy in the transmit direction will depend on the square of the number of hydrophones used – significantly extending the range. Using hydrophone array also has the advantage that would allow precise calibration of existing and planned acoustic telescopes.

Recent studies have predicted the acoustic bipolar pulse generated for the neutrino interaction with in the water at a frequency of over 23 kHz. This research realizes an 8 hydrophone array calibration for generation of Ultra High Energy neutrino-induced pulses at the frequency of 23 kHz. Signal processing techniques are applied to array hydrophone modeling and experimental data generated in a laboratory water tank are used and compared on the calibration system. An eight channel arbitrary waveform generation module has been built using 16 bit dsPIC digital signal controllers for driving hydrophone array transmitters. The NI PXI-6713 commercial module is used for validation.

IV.2. *METHODOLOGY*

The array calibration development can be classified in three phases. In the first phase, signal processing and measurements in water tank are used for the single hydrophone calibration. The characterisation system of the hydrophones is designed to generate the sought bipolar pulse. In a second phase, the eight transmitters are individually checked and validated for the calibration done. Then, the complete eight hydrophone array is placed in the water tank test with the purpose of studying the bipolar signal amplitude transmitted as function of the tension in the transducer, using both the eight channel PIC module and a commercial module for comparison. In a third phase, the eight hydrophones array is simulated by signal processing where is introduced the real array design side, and the environment conditions (Mediterranean sea attenuation, receiver distance), with the objective of predicting the pattern directivity and shape of the bipolar pulse at the detector, determining the correct 8 hydrophone's array length which could send the signal with the 1 º 'pancake' directivity.

IV.2.1 *Signal processing techniques for hydrophone calibration*

Linear Time Invariant (LTI) signal processing can successfully be used to calibrate hydrophones and that standard signal processing techniques can be used to produce arbitrary acoustic waveforms. The LTI model for a transmit hydrophone consists of three parts: an RC electrical circuit coupled to a set of damped mechanical masses and an impedance matching network to couple the hydrophone to the water. This can be represented either in State Space or as a transfer function.

The output signal response of linear time invariant (LTI) system to any input signal can be determined by using convolution operator [7, 8]. It states that if we know the impulse response h (t) of a system, we can compute the output response y (t) to any input x (t) Alternatively, Fourier and inverse Fourier transforms can be used to transfer between domains (e.g. time to frequency and vice versa). When y (w) is the output response, h (w) is the system function, and x (w) is input signal, as shown in Fig.18.

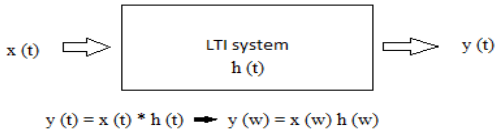

Figure 18. Block diagram of the LTI system to any input signal x(t) .

where y (t) is output impulse response and the symbol * denotes convolution.

Ideally a Dirac delta function would be used as a driving signal as x (ω) =1 and y (ω) =h (ω). In practice however as an impulse or delta function cannot be easily created, a step signal is chosen in order to generate step response of system. The step response of system is the time integral of its impulse response; hence the impulse response can be calculated from differentiation of known step response. As mentioned, the output response signal is resulted from the convolution between input signal and impulse response. Similarly, input signal can be calculated from de-convolution of the output response and system function as shown in (). It is then transferred to the time domain using inverse Fourier transform as shown in (Eq. (8)).

$$x(\omega) = y(\omega)/h(\omega), \quad \frac{1}{2\pi}\int_{-\infty}^{\infty} x(\omega)e^{j\omega t}d(\omega) \tag{8}$$

The method, as described above, has three practical disadvantages. Firstly, the data acquisition needs ahigh signal-to-noise ratio as differentiation is used. Secondly, the step signal input must have a very fast rise time and also high signal to noise ratio. Lastly, the experiment needs to run in large volume or anechoic chamber to avoid reflections. The tank which is available in our workshop has limited volume and reflections soon arrive from the tank boundaries. To avoid the problems which are already mentioned above, signal processing techniques are used. The block diagram of signal processing techniques for calibration is shown in Fig .19.

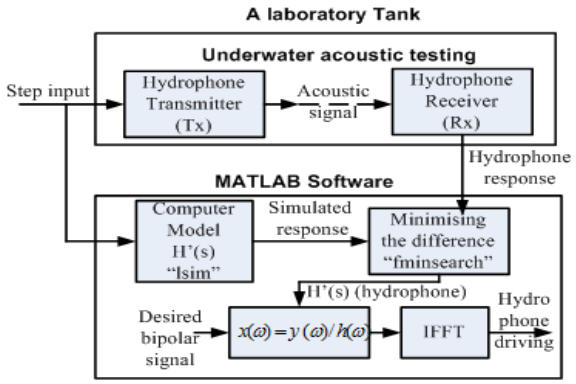

Figure 19. Block diagram of the signal processing techniques used for calibration.

The calibration system is implemented in a rectangular glass water test tank of 1.52 m in length, 0.60 m in width and 0.60 m in depth. The eight hydrophones under calibration are identical robust spherical reference hydrophones (RESON TC 4033) used as transducers to transmit the desired acoustic signals. The RESON TC 4033 provides uniform omni-directional characteristics within the full useable frequency range of 1 Hz to 140 kHz. It has a factory-calibrated transmitting sensitivity of 120 dB ref 1µPa/V@ 1m at 23 kHz.

Matlab computer software is used to create an ideal step signal which is injected to LabVIEW (NI-USB 6211) software, which has a 16 bit analogue-to-digital converter (ADC) sampled at 250 kHz. It is then amplified using a PA94 power amplifier chip (gain of 17) and it's sent out to a single transmitter hydrophone in underwater. The output signal is detected by a wide range bandwidth hydrophone (a Bruel&Kjaer type 8106), general-purpose transducer for making absolute sound measurements over the frequency range from 7 Hz to 80 kHz with receiving sensitivity of -173dB ref 1V/µPa. It provides a flat frequency response and omni-directional characteristics over wide range. The output data from the receiver is the hydrophone step response which is recorded for a data acquisition module (Tektronik TDS 2002 B); it is shown in Fig. 20. in the left panel (a), which is the blue color response.

The know input to the hydrophone, it means the step signal, is injected into the LTI software model and the outputs the real and model hydrophones are matched by reducing the sum squared error (Fig. 20, in hte left panel (a)). The order of the LTI model is gradually increased to ensure sufficient goodness on fit. A fifth-order scaled transfer function (TF) is fitted to this step response (Eq. (9)). The TF is a mathematical representation of the relationship between the input and output of a LTI system.

The input driving signal for 23 kHz bipolar pulse is resulted from replacing fitted transfer function and the desired bipolar signal at 23 kHz. An inverse Fourier transform is then used to convert the input

driving signal from the frequency to time domain (Fig. 20). This is the driving pulse used as input in the hydrophone transmitter to send the 23 kHz bipolar pulse.

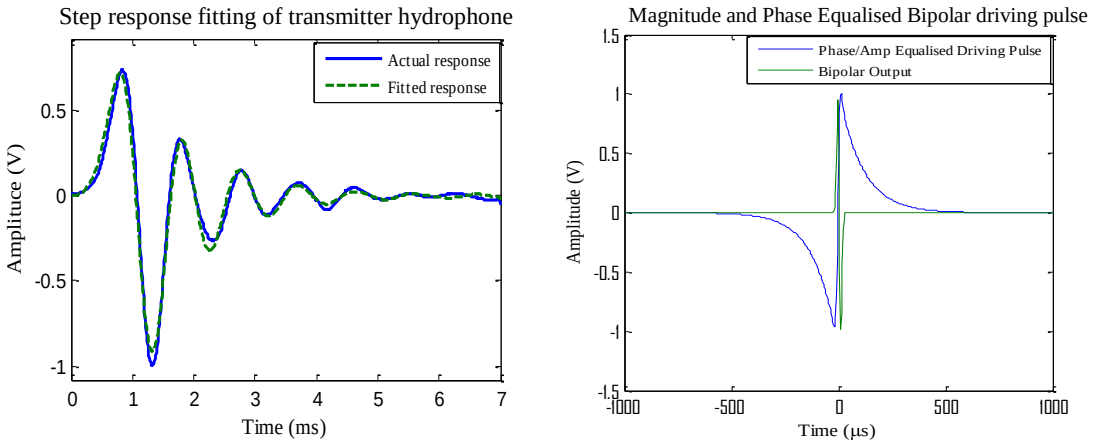

(a) (b)

Figure 20.(a) Fitting the step response simulated with the measured for the hydrophone transfer function;(b) Input driving pulse and output 23 kHz bipolar pulse simulated.

The transfer function $H(s)$ obtained is:

$$\frac{2.436\,s^2 - 0.1226\,s - 0.08506}{0.002913\,s^5 + 0.01982\,s^4 + 0.5279\,s^3 + 2.434\,s^2 + 18.65\,s + 45.9} \quad (9)$$

IV.3. *EXPERIMENTAL SETUP AND RESULTS*

IV.3.1. *Acoustic underwater detection system*

In the experiment, the acoustic underwater detection system comprises of the dsPIC 8 channel arbitrary waveform generator, a National Instruments PXI-6713 8 channel commercial high speed analog output, an eight channel power amplifier, eight TC4033 transmitter hydrophones, a B&K-8106 received hydrophone, a B&K-2690 conditioning amplifier and data acquisition modules (TDS2002B storage oscilloscope, NI PCI-6254 16 bit resolution commercial data acquisition). The block diagram of acoustic underwater detection and the real system at the laboratory are illustrated in Fig. 21and Fig, 22 respectively.

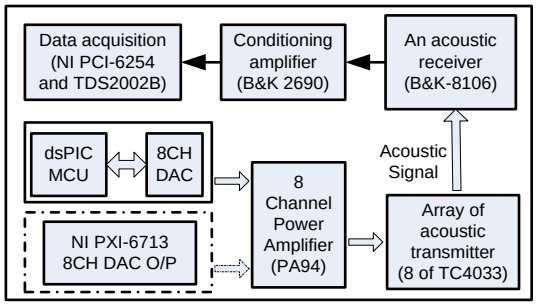

Figure 21.Block diagram of acoustic underwater detection.

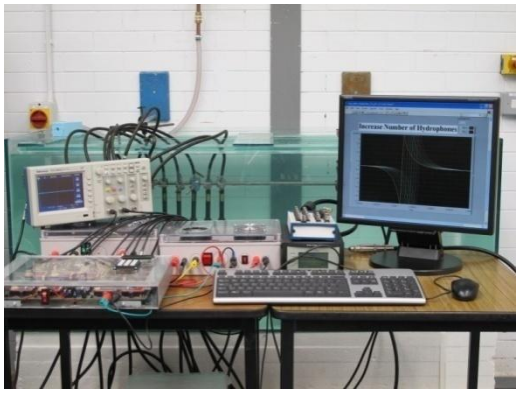

Figure 22. Acoustic underwater detection at the laboratory.

The 60x152x60 cm^3 water tank is used for experiment of the acoustic array at the laboratory. Due to the limitation of dimension of water tank, the hydrophone array is installed in horizontal direction in order to test in along the longest dimension. The water tank and hydrophone installation are illustated in Fig 23.

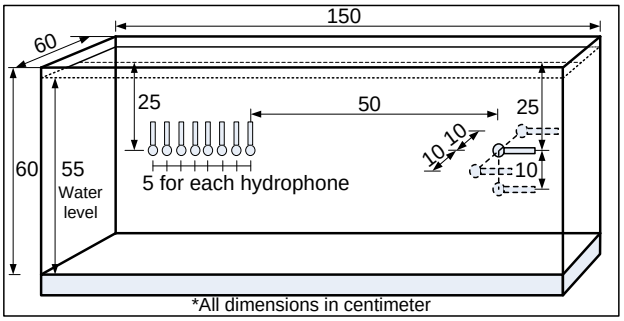

Figure 23. Dimension of water tank and hydrophone installation.

IV.3.2. *Hydrophone array calibration*

The first experiment is the calibration of each hydrophone using the same driving pulse and distance. The signal output voltage from dsPIC and NI PXI-6713 are set to 4.1 V. The driving pulse is then amplified by power amplifier with a gain of 17. The pulse height after the power amplifier is about 70 V which is sufficient to drive the hydrophones in the laboratory and the field.

The testing for calibration of hydrophone is started with dsPIC module. Hydrophone number 1 (H1) is firstly tested and then H2 is also tested but uses the same distance (30 cm between transmitter and receiver) with H1. The received bipolar signals from H1 to H8 are plotted in the Fig. 24 The plot starts from H1 signal in the left hand side until the H8 signal in the right hand side. The hydrophones are extremely well matched.

The NI PXI-6713 is also used to calibrate hydrophones to validate the result with dsPIC module. The regular calibration is done as same as the dsPIC module at the same distance. The result of received signal using PXI-6713 is plotted in Fig. 25.

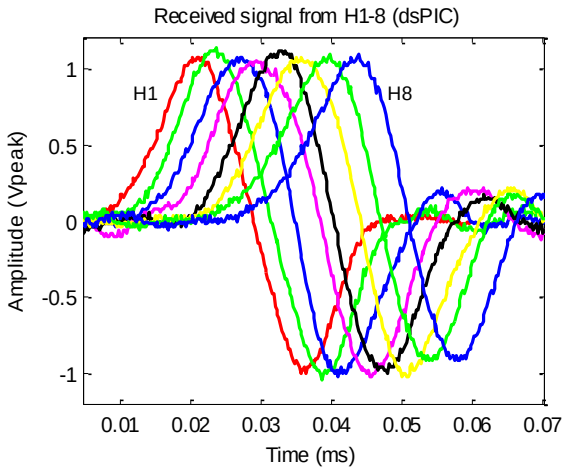

Figure 24. Results of regular calibration for the eight hydrophones with the dsPIC module.

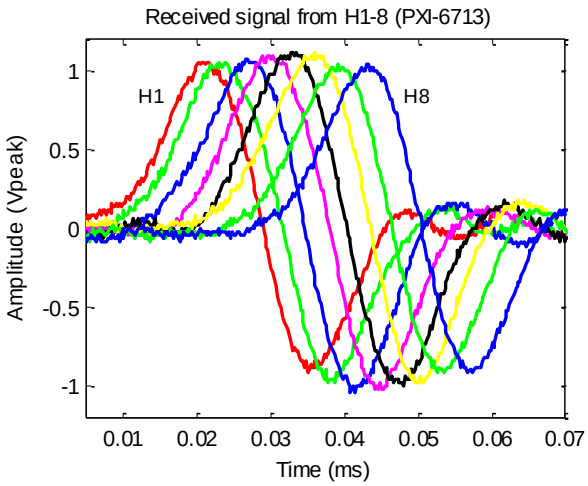

Figure 25. Results of regular calibration for the eight hydrophones with NI PXI-6713.

IV.3.3. *Hydrophone array test and prediction*

The second experiment is the study of the hydrophone array operation, in order to understand the direction and shape of the signals at the receiver. In this experiment, the receive hydrophone is set at three positions. The first position is directly set to the centre of hydrophone transmitters (0 degree of pancake direction). Another two positions are set in the left and bottom side with 10 cm from the centre point to examine off axis behavior. The three positions of received hydrophone is illustrate in Fig 26.

The measurements start with setting hydrophone receiver at the centre point. A bipolar signal is individually sent from hydrophone number 1 (H1) until hydrophone number 8 (H8) to know the amplitude of received signal for each hydrophone.

In the next step, signals from H1-H8 are simultaneously sent to the receiver. In this step, it is very important to set the delay time between each hydrophone transmitter to synchronize the pulses at the receiver. As the distance between hydrophones are 5 cm, and the velocity of sound in water approximately 1500 m/s, the delay time is set to 33.3 μs.

The measurements are repeated with the same procedure but the receiver is moved to the left and bottom points. The PXI-6713 is also tested with the same step to validate the result with dsPIC module. The result data from measurements is recorded in Table 4.

The measurement values are presented that the case of sending eight hydrophones at the centre position can achieve a highest value because it is the best synchronous position of eight signals when compares to the left and bottom positions. These are displayed in Table 4. If the hydrophones were truly

omni-directional then the "Left" and "bottom" column should show identical values. The variations are however slight being of the order of a few percent.

Moreover, in the case of individual sending hydrophone at the centre position, the results show the relation between the falls off sound amplitude with the distance. The relative pressure amplitude and relative distance of each hydrophone position on the experiment is compared with the theoretical model (1/r α pressure). The comparison of relation between pressure and distance of data from theory, dsPIC and PXI-6713 modules is plotted in Fig. 27.

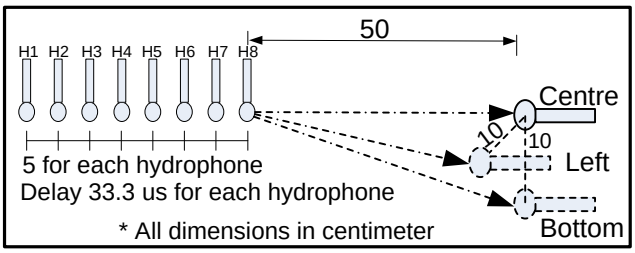

Figure 26. Three positions of received hydrophone.

No of Hydrophone	PXI-6713 module			dsPIC module		
	Centre	Left	bottom	Centre	Left	bottom
H1	1.54	1.46	1.56	1.68	1.54	1.58
H2	1.64	1.60	1.66	1.76	1.62	1.60
H3	1.84	1.76	1.74	1.86	1.74	1.72
H4	1.98	1.84	1.80	1.96	1.92	1.86
H5	2.30	2.06	2.08	2.30	2.04	2.10
H6	2.46	2.24	2.30	2.48	2.22	2.30
H7	2.56	2.28	2.36	2.58	2.30	2.32
H8	2.86	2.64	2.78	2.88	2.70	2.74
H1-8	16.4	15.0	15.8	16.6	14.8	16.00
	*All units are in Vp-p					

Table 4. Comparision received signal between dsPIC and ni pxi-6713 modules

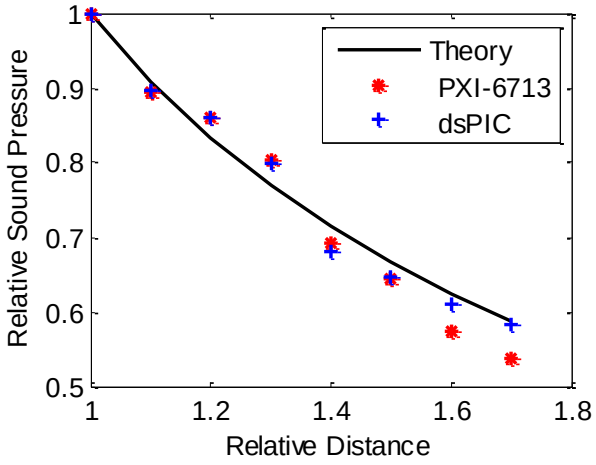

Figure 27. The relation between distance and pressure.

The Fig. 28 shows the received signal at the centre point by increase the number of hydrophone transmitters from two hydrophones until eight hydrophones (lowest amplitude to highest amplitude). The graph is shown that received signals are determined by addition received signal amplitude of each hydrophone.

The comparison of received signal between dsPIC and PXI module for 8 hydrophones is plotted in Fig. 29. The receiver is placed in the centre. The result shows that it is little different between the signal which come from dsPIC and PXI modules.

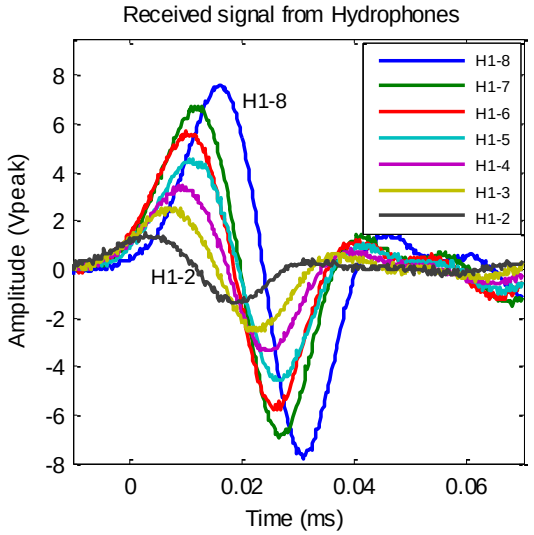

Figure 28.Bipolar pulse receptions from two till eight hydrophones emitting.

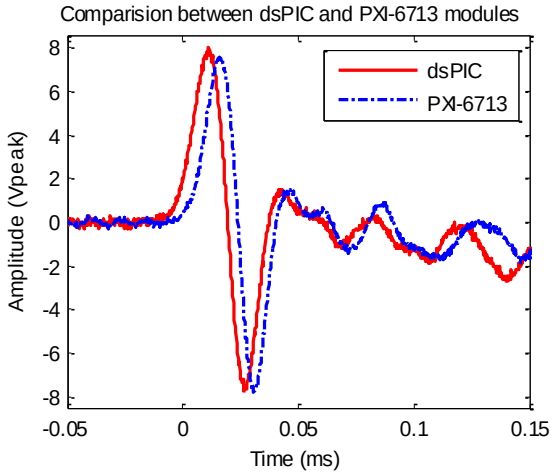

Figure 29. The comparsion received signal between dsPIC and PXI module by 8 hydrophones.

The complete 8 array hydrophone has been checked getting 8 times more amplitude than with a single hydrophone. This confirms that the array can send 556.6 Pa at 1 meter, which corresponds to bipolar pulse pressure amplitude of 225.3 mPa at the AMADEUS system without attenuation.

The ACORNE method of computing the natural complex attenuation presents in the seawater [14] is an accurate tool to predict the 23 kHz bipolar pulse amplitude at the AMADEUS system, which is 2475 m depth. The Fig. 30 shows it for a pressure of 1 Pa:

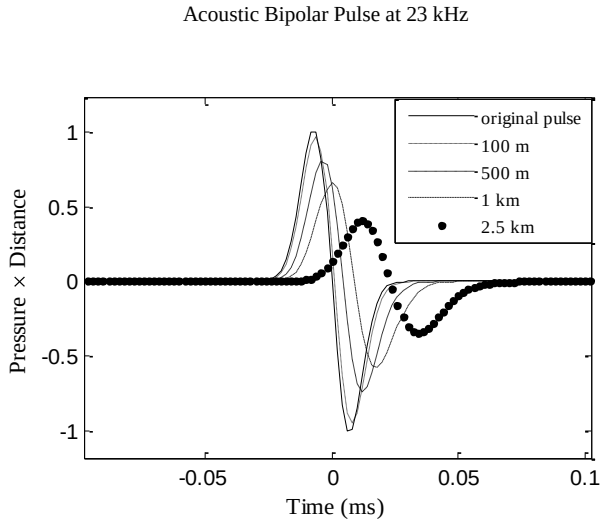

Figure 30. Simulation of the neutrino UHE attenuation with the distance increase in the Mediterranean Sea using ACORNE method

The bipolar pulse amplitude at 23 kHz and 2475m of depth is attenuated 0.5785 Pa per 1 Pa (attenuation of 0.4215 or -7.5dB), moreover the signal has a phase shift, which slightly distorts the pulse. Hence the hydrophone array signal would arrive at the AMADEUS system with about 95 mPa of pressure amplitude with attenuation of the Mediterranean Sea conditions. Taking, the AMADEUS system can detect a signal of 20 mPa at calm sea in the frequency range from 1 to 50 kHz [2], into consideration, and knowing the environment of the Mediterranean Sea is normally mild, the amplitude pressure of 95 mPa should be adequate to be detected by the AMADEUS system sensors.

IV.4. *ACOUSTIC ARRAY SIMULATION*

IV.4.1. *Introduction*

Computing methods of acoustic signal for neutrino shower simulation and the calculation of the sound signal in water at the detector have been described in previous papers [14, 16]. The program allows to be generated in the medium over a wide range of energy (10^5–10^{12} GeV).

The computing method of ACORNE collaboration which includes the complex attenuation effect in the sea water is assumed to simulate the 8 hydrophone array system. It is used to study the array design and size in order to achieve the best approximation to the UHE neutrino-induced pulses properties in the transmission of the artificial bipolar signal pulse. It is referenced to the bipolar pulse signal shape and directivity at the acoustic receiver sensors belonged to the ANTARES system.

IV.4.2. *Array simulation modelling*

For the simulation, is generated a shower parameters as a function of energy, these are stored in a matrix of radial and longitudinal distributions. From the shower parameter matrix a number of points are thrown by a Monte Carlo, the points are generated in polar coordinates. For the array shower the points are split in 8 sphere storey (number of array hydrophones). The acoustic integrator, which works in Cartesian coordinates, calculates the pressure as a scaled derivative histogram of the flight times to the observer [14,16].

The neutrino creates a hadronic shower of approximately 10 m in length and 5 cm in radius. For the simulation, the deposited energy is binned in a cylinder of 10 meters in length and 2.5 cm in width which

gives approximated characteristics to the bipolar signal created for the neutrino interaction, referred to bipolar pulse shape and directivity. This is used as reference to compare it with the array shower generation, which uses the same side as the cylinder simulation but it is split in 8 spheres with equitable centres along the 10 meters in length. The length is also compared for 8 and 6 meters in order to study the length with the most approximation in shape and 'pancake' angle of neutrinos bipolar pulse.

In the coordinate system is chosen such that the neutrino interacts at the origin and travels vertically along the *z* axis where the value of *z* increases with depth and the origin. The point (0, 0,-*Zp*) is chosen such that the maximum 'pancake', it is the point at 0°. The values of *Zp* is energy dependent varying from approximately 460cm (10^5 GeV) to 780cm (10^{12} GeV). The radial distribution gets broader with the age (depth) of the shower; the earlier part contributes more to the pulse energy than the later part of the shower. A fit to seawater data yields a relationship to determine *Zp* from the position of the shower centroid (*Zc*) or from the primary energy *E* (in GeV):

$$z_p = 1.05 z_c - 0.874 \tag{10}$$

$$z_p = -0.046(\log_{10} E)^2 + 1.3\log_{10} E - 0.84 \tag{11}$$

For the analysis the observer is positioned at 2475m from the shower in the centre of the acoustic pancake along the *x* axis, simulating the deployment at the ANTARES detector, the array simulation system for 8 meters length shower is shown in Fig. 31. As the previous publish results have shown [14], the spread of the pancake decreases increasing shower energy. For the simulation, a 10^{11} GeV shower energy deposition is chosen, which was used in previous studies for comparison.

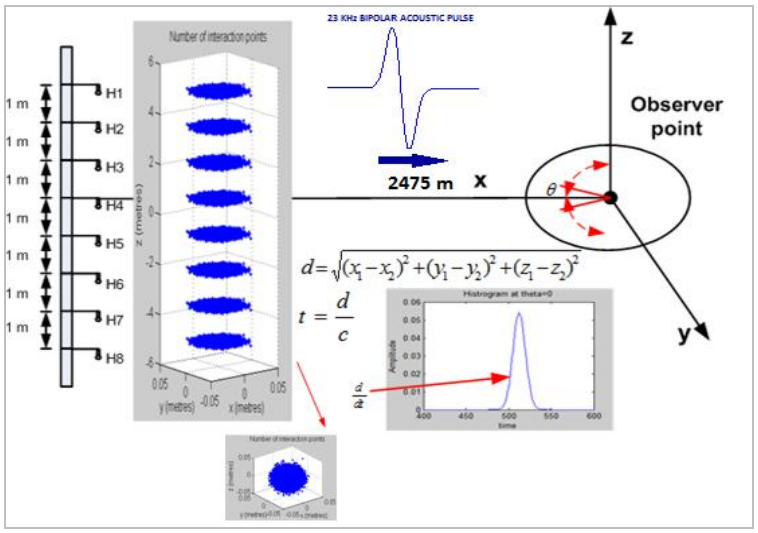

Figure 31.Simulation of the 8 hydrophone array transmission to ANTARES system.

IV.4.3. *Comparison and results*

The array has been analysed with the simulation to know the proper length with what is obtaining the most directive angle maintaining the bipolar pulse shape. An energy equivalent to a 10^{11} GeV shower is shared between eight-spheres for a 6, 8 and 10 meters array length and also a uniform energy distribution along a 10 meter cylinder is shown for comparison. The observer is at 2475m and the result shown in Fig. 32, which gives the pulse energy at the detector vs angular spread of the pancake between 0° and 1°. The pancake spread decreases with array length. The pressure amplitude of the bipolar signal as a function of time for the eight-sphere array with 8 m from 0° to 1°, again for a 10^{11} GeV energy deposition, is shown in Fig. 33. The figure shows that bipolar pulse shape as a function of angle for the 8 m eight-sphere array, imitate properly the behaviour the UHE neutrino acoustic pulse.

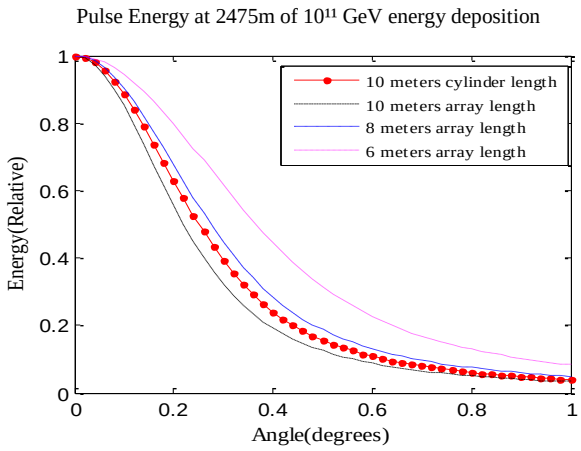

Figure 32. Energy per angle at 2475 meters from 10^{11} GeV of thermal energy shower deposition, under Mediterranean Sea condition.

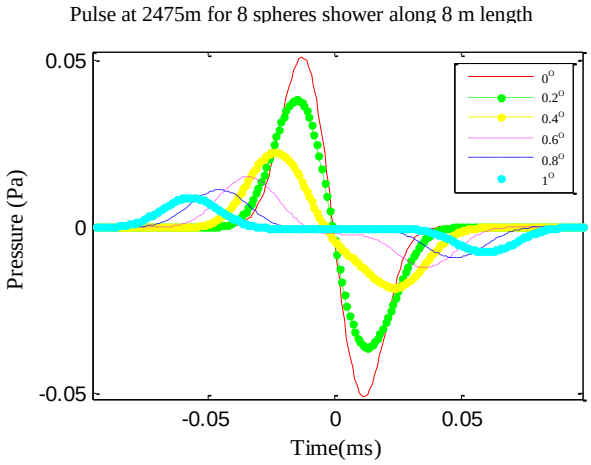

Figure 33. Amplitude (Pa) in time (ms) of the Acoustic bipolar pulse generated from a 10^{11} GeV thermal energy shower deposition at 2475 meters under Mediterranean Sea conditions(array shower simulation of 8 meters length).

IV.4. *CONCLUSIONS*

The acoustic hydrophone array calibration has been developed for UHE neutrino detection using the combination and comparison of signal processing techniques and experimental data generation, showing excellent agreement. The linear hydrophone array simulation shows that the eight hydrophones arranged over an eight meters spacing structure can mimic the anticipated pancake behaviour predicted from neutrino induced showers as well as the acoustic bipolar pulse shape and amplitude at the ANTARES system.

The 8 channel arbitrary waveform generation module using dsPIC microcontrollers has been developed for acoustic underwater detection. The dsPIC module and NI PXI-6713 commercial module give very similar results.

In future work, the array system calibrated is expected to be placed in a structure of 8 meters length according with the simulated results and it will be used at sea sites to send the acoustic bipolar signal for UHE neutrinos detection at the ANTARES system in September of 2011. The 8 channel PIC hydrophone array module built will be used for controlling and processing during the deployment.

This work has been accepted for the MARSS – IEEE MASS 2011 Conference [32]

ACKNOWLEDGEMENTS

I would like to thank professors and colleagues M. Ardid, S. Danaher, W. Ooppakaew and J.Martínez-Mora for helping me to carry out this project.

Also I would like to thank to the Erasmus Programme of the European Union and the MULTIDARK Consolider who funs part of this project.

And finally to my family and friends who are always giving me energies to keep everything on, specially to my mother.

REFERENCES

[1] J.A.Aguilar, *ANTARES:The first undersea neutrino telescope*. Nucl.Instr. and Meth.A (2011), [arxiv:1104.1607v1].

[2] J.A.Aguilar, *AMADEUS:The Acoustic neutrino detection system of the ANTARES Deep-Sea neutrino telescope*, Nucl.Instr. and Meth.A (2010),doi:10.1016/j.nima.2010.09.53,arXiv:1009.4179.

[3] K.Shin,J.K.Hammond, *Fundamentals of signal Processing for sound and Vibration Engineers*, John Wiley & Sons,Ltd (2008).

[4] S. Danaher, *First data from ACoRNE and signal processing techniques*, Journal of Physics: Conference Series., vol. 81, pp.1-5, 2007.

[5] L. F. Thompson, *Future plans for the ACoRNE collaboration*, Journal of Physics: Conference Series., vol. 81, pp. 1-5, 2007.

[6] R. Nahnhauer and S. Böser, *Proceedings of the International Workshop on Acoustic and Radio EeV Neutrino detection Activities (ARENA)*, World Scientic (May 2005). L.Thompson and S. Danaher.*Proceedings of the Workshop on Acoustic and Radio EeV Neutrino detection Activities (ARENA)*, (June 2006). Journal of Physics: Conference Series 81 (2007).

[7] E. Andres, Astropart *The AMANDA neutrino telescope: principle of operation and first results*. Astropart. Phys. 13 (2000) 1-20;http://arxiv.org/abs/astro-ph/9906203.

[8] A. Achterberg, *First Year Performance of the Icecube NeutrinoTelescope*, Astropart. Phys. 26 (2006) 155-173;http://arxiv.org/abs/astro-ph/0604450.

[9] G. Aggouras, *Operation and performance of the NESTOR test detector*, Nucl. Instrum. And Meth. A 552 (2005) 420-439.

[10] E. Migneco,*Recent achievements of the NEMO project*, Nucl. Instrum. and Meth. A 588 (2008) 111-118.

[11] E. de Wolf, KM3NeT, *A new generation neutrino telescope*, Nucl. Instrum. and Meth. A 588 (2008) 86-91.

[12] V. Aynutdinov, *The Baikal neutrino experiment: Status, selected physics results, and perspectives*, Nucl. Instrum. and Meth. A 588 (2008) 99-106.

[13] J. G. Learned, *Acoustic Radiation By Charged Atomic Particles In Liquids: An Analysis*, Phys. Rev. D 19, (1979) 3293.

[14] S.Bevan, *Study of the acoustic siganture of UHE neutrino interactions in water and ice*, Nucl.Instr. and Meth.A 607 (2009) 398-411.

[15] G. A. Askaryan, *Sov. J. Atom Energy* **3**, 921 (1957).

[16] S. Bevan, *Simulation of Ultra High Energy Neutrino Interactions in Ice and Water*. Astroparticle Physics 28 (2007) 366–379.

[17] R. E. Francois, G. R. Garrison, *Sound absorption based on ocean measurements: Part I:Pure water and magnesium sulfate contributions*, Journal of the Acoustical Society of America 72(3) (1982) 896-907. R. E. Francois, G. R. Garrison, *Sound absorption based on ocean measurements: Part II:Boric acid contribution and equation for total absorption*, Journal of the Acoustical Society of America 72(6) (1982) 1879-1890.

[18] M. A. Ainslie and J. G. McColm, A *simplified formula for viscous and chemical absorption in seawater*, Journal of the Acoustical Society of America 103(3) (1998) 1671-1672.

[19] L. N. Lieberman, The *Origin of Sound Absorption in Water and in Sea Water*, The Journal of the Acoustical Society of America 20(6) (1948) 868-873.

[20] V. Niess and V. Bertin, *Underwater Acoustic Detection of Ultra High Energy Neutrinos*, Astropart. Phys. 26(4-5) (2006) 243-256;http://arxiv.org/abs/astro-ph/0511617.

[21] P.Keller, *Acoustic Positioning system for the Deep-Sea ANTARES Neutrino telescope*, sensorcomm, pp243-247 (2007).

[22] C. Naumann, *Proc. of the Int. Workshop (ARENA 2005)*, World Scientific Publishing, Singapore (2006) 92; preprint: arXiv:astro-ph/0511243.

[23] C. Naumann, Ph.D. Thesis, Univ. Erlangen-Nürnberg, FAU-PI4-DISS-07-002, 2007.

[24] K. Graf, Experimental *studies within ANTARES towards acoustic detection of ultra-high energy neutrinos in the deep sea*, Ph.D. thesis, Univ. Erlangen-N¨urnberg, 2008, FAU-PI1-DISS-08-001.

[25] R.J. Urick, *Ambient Noise in the Sea*, Undersea Warfare Tech. Office, Naval Sea and Systems Command,Dept. of the Navy, Washington, D.C(1984).

[26] M. Neff, *Studie zur akustischen Teilchendetektion im Rahmen des ANTARES-Experiments: Entwicklung und Integration von Datennahmesoftware*, Diploma thesis, Univ. Erlangen-N¨urnberg, 2007, FAU-PI1-DIPL-07-003.

[27] M.Bou-Cabo, PhD. Thesis: *Acoustics for underwater neutrino telescopes*. Universidad Politécnica de Valencia(2011.01).

[28] M. Ardid, S.Adrian, et. at. *R&D studies for the development of a compact transmitter able to mimic the acoustic signature of a UHE neutrino interaction*. Nucl. Instr. and Meth. A (2010), doi:10.1016/j.nima.2010.11.139.

[29] W. Ooppakaew,S. Danaher, Hydrophone Calibration Based on Microcontrollers for Acoustic Detection of UHE Neutrinos. Nucl.Instr. and Meth.A (2011),doi:10.1016/j.nima.2010.11.142.

[30] S. T. Karris, *Signals and Systems with MATLAB Applications*,California: Orchard Publications(2003).

[31] V. K. Ingle, J. G. Proakis, *Digital Signal Processing Using MATLAB.* USA: Bookware Companion Series (2007).

[32] W.Ooppakaew, S.Danaher, M.Saldaña, *Acoustic Array Calibration and Signal Processing for UHE Neutrinos Generation*, MARSS 2011. Northumbria University and Universidad Politécnica de Valencia,

APPENDIX

Appendix 1. Matlab code with the fynal system application for the received signal análisis from the AMADEUS-ANTARES positioning system.

```
clear all
clc
close all

%% ------------- *******   APLICABLE DEL SENSOR 6 al 9 ********  --------- %%
[x,fs,bits]=wavread('sensor7.wav'); % x: muestras de la señal en el
tiempo,fs:frecuencia de muestreo,bits=número de bits para codificar 1 muestra
fs
ts=1/fs
bits

s=7;%NUM SENSOR (para plots)
I=0.15*0.25;                                                    % inicio
(muestras) señal 1° recepción
F=0.15*0.05;                                                   %
final(muestras) señal 1° recepción
%tamaño(muestras) total 1° recepción
fin1=300000;


num_muestrasI=zeros;
num_muestrasF=zeros;
cont1=1;
```

```
cont=1;
% ------------------------------ RECEPCIÓN 1 a la 11 ----------------------
-  %
            % ------------------  ENVOLVENTE  ------------------%
      hilbert=hilbert(x);
envelopeH=abs(hilbert);

for i=1:1:11

   % -------------------  Deteccion de cada senyal ----------------   %
    if i>=2

    cont2=1;
    cont3=1;

ini(i)=ini_r(i-1)+150000;
fin(i)=fin_r(i-1)+220000;

for j=ini(i):1:fin(i)                                                  %for
desde inicio hasta un margen asegurado de la recepción de la 1
señal:300000*Ts=1.2segundos
 if x(j)>I
     num_muestrasI(cont2)=j;
     cont2=cont2+1;%asi conocemos en qué muestra esta el inicio de la 1
recepción
                                          % dejamos un margen desde el
inicio para asegurar que campte la amplitud correspondiente a la finalizacion
de la señal
 end
end
ini_r(i)=num_muestrasI(1);%asi coge la primera muestra que ha captado >= que
I
  ini_fin=ini_r(i)+500;

 for k=ini_fin:1:fin(i)
     if x(k)<=F & x(k)>0 %La condición de x(i)>0 , ya que, sino cogia números
negativos de la señal x
         num_muestrasF(cont3)=k;
         cont3=cont3+1;
     end
 end

 fin_r(i)=num_muestrasF(1);%asi coge la primera muestra que ha captado <= que
F
    else

    cont2=1;
    cont3=1;

     for j=1:1:fin1
        %for desde inicio hasta un margen asegurado de la recepción de la 1
señal:300000*Ts=1.2segundos
 if x(j)>I
     num_muestrasI(cont2)=j;
```

```
     cont2=cont2+1;%asi conocemos en qué muestra esta el inicio de la 1
recepción                                          % dejamos un margen desde el
inicio para asegurar que campte la amplitud correspondiente a la finalizacion
de la señal
 end
end
ini_r(i)=num_muestrasI(1);%asi coge la primera muestra que ha captado >= que
I
  ini_fin=ini_r(i)+500;


 for k=ini_fin:1:fin1
     if x(k)<=F & x(k)>0 %La condición de x(i)>0 , ya que, sino cogia números
negativos de la señal x
         num_muestrasF(cont3)=k;
         cont3=cont3+1;
     end
 end

 fin_r(i)=num_muestrasF(1);%asi coge la primera muestra que ha captado <= que
F



    end

     %-------------- Calculo de la amplitud propia de la señal ------------%



 for l=(ini_r(i)-100):1:fin_r(i)
 %muestras de ini y fin de r1

   z(l)=envelopeH(l);

 end

 ts=1/fs;

rango_estable=envelopeH(ini_r(i)+100:fin_r(i)-100);
 amplitud(i)=mean(rango_estable);

I=amplitud(i)*0.25;                                                        %
inicio (muestras) señal 1° recepción
F=amplitud(i)*0.3;

for p=1:1:fin1                                                    %for desde
inicio hasta un margen asegurado de la recepción de la 1
señal:300000*Ts=1.2segundos
 if x(p)>=I
     num_muestrasI(cont1)=p;
     cont1=cont+1;%asi conocemos en qué muestra esta el inicio de la 1
recepción
```

```
                                                % dejamos un margen desde el
inicio para asegurar que campte la amplitud correspondiente a la finalizacion
de la señal
 end
end
ini_r(i)=num_muestrasI(1);%asi coge la primera muestra que ha captado >= que
I
  ini_fin=ini_r(i)+500;

 for q=ini_fin:1:fin1
     if x(q)<=F & x(q)>0 %La condición de x(i)>0 , ya que, sino cogia números
negativos de la señal x
         num_muestrasF(cont)=q;
         cont=cont+1;
     end
 end

 fin_r(i)=num_muestrasF(1);%asi coge la primera muestra que ha captado <= que
F

                                                 %creamos el nuevo vector para
que posteriormente guarde la señal recibida 1ª entre los margenes del eje
horizontal correctos
 ini_analisis(i)=ini_r(1);
 ini_analisis(i)=ini_r(i)-200;
 fin_r(i)=fin_r(i)+150;
 %z=x(ini_r1:1:fin_r1);
for l=ini_analisis(i):1:fin_r(i)

    za(l)=x(l);
   hilbert1(l)=hilbert(l);
    envelopeH1(l)=envelopeH(l);
end


%*************************************************************%
%****** Filtrado Paso-Banda ***************%
%*************************************************************%


%******** Transformada de Fourier de la señal  ************%

t=[ini_analisis(i):1:fin_r(i)].*ts; %rango temporal de la señal
f=1./(t.*ts);%rango frecuencial de la señal

N=length(za(ini_analisis(i):fin_r(i)));%longitud de la señal
frec =[(-1/ts)/2:(1/ts)/(N-1):((1/ts)/2)];%rango frecuencial de la
tranformada

z1a= fftshift(fft(za(ini_analisis(i):fin_r(i))));
figure,subplot(1,2,2),plot(t,za(ini_analisis(i):fin_r(i))),title(['Señal'
num2str(i) '-Sensor' num2str(s) '- : Onda en tiempo'])
subplot(1,2,1),plot(frec,z1a),title(['Señal' num2str(i) '-Sensor' num2str(s)
'- : Onda en frecuencia(transformada)'])
```

```
%********* Detección de la Frecuencia de la señal, Fp y Fs *******%

m=max(z1a)
p=find(z1a==m) %En el punto donde capta el pico en la transformada se
encuentra su frecuencia

frec_senyal=frec(p);
%por si coge el valor máximo(correspondiente a la frecuencia) en la parte
%imaginaria, quitarle el valor negativo:
if frec_senyal<0
    frec_senyal=-frec_senyal
else
   frec_senyal=frec_senyal
end




%-------- Aplicamos Filtro Paso Banda de 35 a 65 KHz a una frecuencia de unos
60KHz ---- %



  fp_min=40000;%fpass minimo
fp_max=60000;%fpass maximo
fs_min=35000;%fstop minimo con 2.5KHz  de margen
fs_max=65000;%fstop maximo con 2.5KHz de margen


Wp = [fp_min fp_max]/fs;%Frecuencias que deseas pasar
Ws = [fs_min fs_max]/fs;%Tolerancia que ofreces a la horquilla de frecuencias
Rp = 1; Rs = 10;%Tolerancias de la banda de rizado
[n,Wn] = buttord(2*Wp,2*Ws,Rp,Rs)%Definicion
[b,a] = butter(n,Wn);
figure,freqz(b,a,bits,fs)%Parametros y ordenes del filtro + numero de puntos
+ Frecuencia de muestreo
title(['Butterworth Bandpass Filter  '  num2str(fp_min) 'Hz - '
num2str(fp_max) 'Hz' ])

    zaf1(ini_analisis(i):fin_r(i))=
filter(b,a,za(ini_analisis(i):fin_r(i)));%aplicamos filtro a la señal
z1af1= fftshift(fft(zaf1(ini_analisis(i):fin_r(i))));

figure,subplot(1,2,1),plot(frec,z1af1),title(['ondafiltrada' num2str(i)
'F.Paso Banda (frecuencia):  '  num2str((fp_min)) 'Hz - ' num2str(fp_max)
'Hz' ]);
subplot(1,2,2),plot(t,zaf1(ini_analisis(i):fin_r(i))),title(['ondafiltrada'
num2str(i) 'F.Paso Banda (tiempo):  '  num2str((fp_min)) 'Hz - '
num2str((fp_max)) 'Hz' ]);

% ---- Aplicamos filtro Banda Paso entre 40-60KHz a la hilbert senyal -----%
  % --- para obtener la envolvente de la senyal filtrada  ----  %
```

```
hilbert1=hilbert1(ini_analisis(i):fin_r(i));
filtro_h(ini_analisis(i):fin_r(i))= filter(b,a,hilbert1);



%********* Detección de la Frecuencia de la señal de nuevo , Fp y Fs *******%
m=max(z1af1)
p=find(z1af1==m) %En el punto donde capta el pico en la transformada se
encuentra su frecuencia

frec_senyal=frec(p);
%por si coge el valor máximo(correspondiente a la frecuencia) en la parte
%imaginaria, quitarle el valor negativo:
    if frec_senyal<0
    frec_senyal=-frec_senyal
    else
   frec_senyal=frec_senyal
    end


fp_min=frec_senyal-2500%fpass minimo con 2.5KHz de margen desde la frecuencia
propia
fp_max=frec_senyal+2500%fpass maximo 2.5KHz de margen desde la frecuencia
propia
fs_min=fp_min-10000%fstop minimo con 10KHz  de margen desde la frecuencia
propia
fs_max=fp_max+10000%fstop maximo con 10KHz de margen desde la frecuencia
propia


%---------- Rango de Banda de paso de margen  5KHz  con frec
central=frecuencia de la señal  ------%

Wp = [fp_min fp_max]/fs;%Frecuencias que deseas pasar
Ws = [fs_min fs_max]/fs;%Tolerancia que ofreces a la horquilla de frecuencias
Rp = 1; Rs = 10;%Tolerancias de la banda de rizado
[n,Wn] = buttord(2*Wp,2*Ws,Rp,Rs)%Definicion
[b,a] = butter(n,Wn);
figure,freqz(b,a,bits,fs)%Parametros y ordenes del filtro + numero de puntos
+ Frecuencia de muestreo
title(['Butterworth Bandpass Filter  '  num2str(fp_min) 'Hz - '
num2str(fp_max) 'Hz' ])

y(ini_analisis(i):fin_r(i))= filter(b,a,zaf1(ini_analisis(i):fin_r(i)));
ondafiltrada = fftshift(fft(y(ini_analisis(i):fin_r(i))));

figure
subplot(1,2,1),plot(frec,ondafiltrada),title(['ondafiltrada' num2str(i)
'(frecuencia):  '  num2str(fp_min) 'Hz - ' num2str(fp_max) 'Hz' ]);
subplot(1,2,2),plot(t,y(ini_analisis(i):fin_r(i))),title(['ondafiltrada'
num2str(i) '(tiempo):  '  num2str(fp_min) 'Hz - ' num2str(fp_max) 'Hz' ]);
```

```
figure,subplot(2,2,2),plot(t,za(ini_analisis(i):fin_r(i))),title(['Señal'
num2str(i) '-Sensor' num2str(s) '- : Onda en tiempo'])
subplot(2,2,1),plot(frec,z1a),title(['Señal' num2str(i) '-Sensor' num2str(s)
'- : Onda en frecuencia(transformada)'])
subplot(2,2,3),plot(frec,ondafiltrada),title(['ondafiltrada' num2str(i)
'(frecuencia):  '  num2str(fp_min) 'Hz - ' num2str(fp_max) 'Hz' ]);
subplot(2,2,4),plot(t,y(ini_analisis(i):fin_r(i))),title(['ondafiltrada'
num2str(i) '(tiempo):  '  num2str(fp_min) 'Hz - ' num2str(fp_max) 'Hz' ]);

figure
set(gca,'fonts',8)
plot(frec,z1a,frec,z1af1,frec,ondafiltrada),title(['SENSOR' num2str(s)
'OndaFiltrada' num2str(i) '(frecuencia)  Paso Banda a Frec.Central:  '
num2str(frec_senyal) 'Hz - '])
legend('S. Original' ,'S. F.P.B 40-60KHz','S. F.P.B Margen 5KHz')


figure
set(gca,'fonts',8)
plot(t,za(ini_analisis(i):fin_r(i)),t,zaf1(ini_analisis(i):fin_r(i)),t,y(ini_
analisis(i):fin_r(i))),title(['SENSOR' num2str(s)  'OndaFiltrada' num2str(i)
'(tiempo)  Paso Banda a Frec.Central:  ' num2str(frec_senyal) 'Hz - '])
legend('S. Original' ,'S. F.P.B 40-60KHz','S. F.P.B Margen 5KHz')




pause

% ---------------  Método 'HILBERT TRANSFORM' ----------%

% ---- Aplicamos filtro Banda Paso 5KHz a la hilbert senyal filtrada -----%
  % --- entre 40-60KHz para obtener la envolvente de la senyal filtrada  ----
%

filtro_h= filter(b,a,filtro_h(ini_analisis(i):fin_r(i)));
envelopeH_filtrado(ini_analisis(i):fin_r(i))=abs(filtro_h);


fase=unwrap(angle(filtro_h)); %fase
fx=diff(unwrap(angle(filtro_h)))./diff(t)/(2*pi); %frecuencia



%------------------ amplitud  ------------ %

figure,subplot(3,1,1),plot(t,y(ini_analisis(i):fin_r(i)),t,envelopeH_filtrado
(ini_analisis(i):fin_r(i)),'r:'),title(['SENSOR' num2str(s) ':Muestras y
Envolvente(Mediante HILBERT)de la Señal recibida ' num2str(i) ' en el tiempo
parte estable']);
xlabel('t(segundos)');
ylabel('x(t) normalizado')
grid on
```

```
%------------------ fase  ------------ %
subplot(3,1,2),plot(t,fase),title(['SENSOR' num2str(s) ':Fase de la Señal
recibida ' num2str(i) ' en el tiempo']);
xlabel('t(segundos)');
ylabel('fase (t)')
grid on
%s=[z1 z];
%s=[z za];%Aqui quedan guardadas todas las señales su número de muestras
correspondiente

%------------------ frecuencia  ------------ %
subplot(3,1,3),plot(t(2:end),fx),title(['SENSOR' num2str(s) ':Frecuencia de
la Señal recibida ' num2str(i) ' en el tiempo']);
xlabel('t(segundos)');
ylabel('frecuencia (t)')
grid on
% --------------------  Cálculo del tiempo de subida --------------------%

% Calculamos de nuevo la amplitud, en la señal Filtrada, en la parte central
% de la senyal, ya que, es normalmente, donde tiene un nivel de amplitud
% mas estable


rango_estable=envelopeH_filtrado(ini_analisis(i)+300:fin_r(i)-250);
amplitud(i)=mean(rango_estable)

% ----------------------

y1(ini_analisis(i):fin_r(i))=envelopeH_filtrado(ini_analisis(i):fin_r(i));

a2=amplitud(i)*0.25;
i2=find(y1>=a2);
i2(i)=min(i2);
format long
Ts_25(i)=i2(i)*ts


y1=0;
%---------------------------
% --------------------  Cálculo del tiempo de bajada --------------------%

ini_Tb=ini_analisis(i)+350;
fin_Tb=fin_r(i);%-50?
%asi nos hemos desplazado a la parte final para el cálculo del Tb
y2=envelopeH_filtrado(ini_Tb:fin_Tb);% se tiene que tener en cuenta que el
1°valor de y2 realmente corresponde a la muestra ini_Tb,para el posterior
cálcuo del tiempo

a3=amplitud(i)*0.75;
f3=find(y2<=a3);
f3(i)=min(f3)+ini_Tb;
format long
Tb_75(i)=f3(i)*ts
```

```
duracion_muestras25_75(i)=-f2(i)+f4(i);
duracion_tiempo25_75(i)=(duracion_muestras25_75(i)).*ts;



y2=0;
 pause
end

% ------------------------------ RECEPCIONES 12,13,14,15 -------------------
-----  %

ini_r(11)=4030000;
fin_r(11)=4030520;
%Nos desplazamos al siguiente grupo de recepciones
for i=12:1:15

   % -------------------  Deteccion de cada senyal ----------------   %
    if i>=2

    cont2=1;
    cont3=1;

ini(i)=ini_r(i-1)+150000;
fin(i)=fin_r(i-1)+220000;

for j=ini(i):1:fin(i)                                                    %for
desde inicio hasta un margen asegurado de la recepción de la 1
señal:300000*Ts=1.2segundos
 if x(j)>I
     num_muestrasI(cont2)=j;
     cont2=cont2+1;%asi conocemos en qué muestra esta el inicio de la 1
recepción
                                            % dejamos un margen desde el
inicio para asegurar que campte la amplitud correspondiente a la finalizacion
de la señal
 end
end
ini_r(i)=num_muestrasI(1);%asi coge la primera muestra que ha captado >= que
I
  ini_fin=ini_r(i)+500;

 for k=ini_fin:1:fin(i)
     if x(k)<=F & x(k)>0 %La condición de x(i)>0 , ya que, sino cogia números
negativos de la señal x
         num_muestrasF(cont3)=k;
         cont3=cont3+1;
     end
 end

 fin_r(i)=num_muestrasF(1);%asi coge la primera muestra que ha captado <= que
F
    else
```

```
    cont2=1;
    cont3=1;

     for j=1:1:fin1
        %for desde inicio hasta un margen asegurado de la recepción de la 1
señal:300000*Ts=1.2segundos
 if x(j)>I
     num_muestrasI(cont2)=j;
     cont2=cont2+1;%asi conocemos en qué muestra esta el inicio de la 1
recepción                                          % dejamos un margen desde el
inicio para asegurar que campte la amplitud correspondiente a la finalizacion
de la señal
 end
end
ini_r(i)=num_muestrasI(1);%asi coge la primera muestra que ha captado >= que
I
  ini_fin=ini_r(i)+500;


 for k=ini_fin:1:fin1
     if x(k)<=F & x(k)>0 %La condición de x(i)>0 , ya que, sino cogia números
negativos de la señal x
         num_muestrasF(cont3)=k;
         cont3=cont3+1;
     end
 end

 fin_r(i)=num_muestrasF(1);%asi coge la primera muestra que ha captado <= que
F



    end

     %-------------- Calculo de la amplitud propia de la señal ------------%



 for l=(ini_r(i)-100):1:fin_r(i)
 %muestras de ini y fin de r1

   z(l)=envelopeH(l);

 end

 ts=1/fs;

rango_estable=envelopeH(ini_r(i)+100:fin_r(i)-100);
 amplitud(i)=mean(rango_estable);

I=amplitud(i)*0.25;                                                    %
inicio (muestras) señal 1° recepción
F=amplitud(i)*0.3;
```

```
for p=1:1:fin1                                                    %for desde
inicio hasta un margen asegurado de la recepción de la 1
señal:300000*Ts=1.2segundos
 if x(p)>=I
     num_muestrasI(cont1)=p;
     cont1=cont+1;%asi conocemos en qué muestra esta el inicio de la 1
recepción
                                              % dejamos un margen desde el
inicio para asegurar que campte la amplitud correspondiente a la finalizacion
de la señal
 end
end
ini_r(i)=num_muestrasI(1);%asi coge la primera muestra que ha captado >= que
I
  ini_fin=ini_r(i)+500;

 for q=ini_fin:1:fin1
     if x(q)<=F & x(q)>0 %La condición de x(i)>0 , ya que, sino cogia números
negativos de la señal x
         num_muestrasF(cont)=q;
         cont=cont+1;
     end
 end

 fin_r(i)=num_muestrasF(1);%asi coge la primera muestra que ha captado <= que
F

                                               %creamos el nuevo vector para
que posteriormente guarde la señal recibida 1ª entre los margenes del eje
horizontal correctos
 ini_analisis(i)=ini_r(1);
 ini_analisis(i)=ini_r(i)-100;
 fin_r(i)=fin_r(i)+150;
 %z=x(ini_r1:1:fin_r1);
for l=ini_analisis(i):1:fin_r(i)

    za(l)=x(l);
   hilbert1(l)=hilbert(l);
    envelopeH1(l)=envelopeH(l);
end


%************************************************************%
%****** Filtrado Paso-Banda ***************%
%************************************************************%


%******** Transformada de Fourier de la señal  ************%

t=[ini_analisis(i):1:fin_r(i)].*ts; %rango temporal de la señal
f=1./(t.*ts);%rango frecuencial de la señal

N=length(za(ini_analisis(i):fin_r(i)));%longitud de la señal
```

```
frec =[(-1/ts)/2:(1/ts)/(N-1):((1/ts)/2)];%rango frecuencial de la
tranformada

z1a= fftshift(fft(za(ini_analisis(i):fin_r(i))));
figure,subplot(1,2,2),plot(t,za(ini_analisis(i):fin_r(i))),title(['Señal'
num2str(i) '-Sensor' num2str(s) '- : Onda en tiempo'])
subplot(1,2,1),plot(frec,z1a),title(['Señal' num2str(i) '-Sensor' num2str(s)
'- : Onda en frecuencia(transformada)'])

%********* Detección de la Frecuencia de la señal, Fp y Fs *******%

m=max(z1a)
p=find(z1a==m) %En el punto donde capta el pico en la transformada se
encuentra su frecuencia

frec_senyal=frec(p);
%por si coge el valor máximo(correspondiente a la frecuencia) en la parte
%imaginaria, quitarle el valor negativo:
if frec_senyal<0
    frec_senyal=-frec_senyal
else
   frec_senyal=frec_senyal
end




%-------- Aplicamos Filtro Paso Banda de 35 a 65 KHz a una frecuencia de unos
60KHz ---- %



  fp_min=40000;%fpass minimo
fp_max=60000;%fpass maximo
fs_min=35000;%fstop minimo con 2.5KHz  de margen
fs_max=65000;%fstop maximo con 2.5KHz de margen


Wp = [fp_min fp_max]/fs;%Frecuencias que deseas pasar
Ws = [fs_min fs_max]/fs;%Tolerancia que ofreces a la horquilla de frecuencias
Rp = 1; Rs = 10;%Tolerancias de la banda de rizado
[n,Wn] = buttord(2*Wp,2*Ws,Rp,Rs)%Definicion
[b,a] = butter(n,Wn);
figure,freqz(b,a,bits,fs)%Parametros y ordenes del filtro + numero de puntos
+ Frecuencia de muestreo
title(['Butterworth Bandpass Filter  '  num2str(fp_min) 'Hz - '
num2str(fp_max) 'Hz' ])

    zaf1(ini_analisis(i):fin_r(i))=
filter(b,a,za(ini_analisis(i):fin_r(i)));%aplicamos filtro a la señal
z1af1= fftshift(fft(zaf1(ini_analisis(i):fin_r(i))));
```

```
figure,subplot(1,2,1),plot(frec,z1af1),title(['ondafiltrada' num2str(i)
'F.Paso Banda (frecuencia):  '  num2str((fp_min)) 'Hz - ' num2str(fp_max)
'Hz' ]);
subplot(1,2,2),plot(t,zaf1(ini_analisis(i):fin_r(i))),title(['ondafiltrada'
num2str(i) 'F.Paso Banda (tiempo):  '  num2str((fp_max)) 'Hz - '
num2str((fp_max)) 'Hz' ]);

% ---- Aplicamos filtro Banda Paso entre 40-60KHz a la hilbert senyal -----%
  % --- para obtener la envolvente de la senyal filtrada  ----  %

  %hilbert1(ini_analisis(i):fin_r(i))=
filter(b,1,hilbert1(ini_analisis(i):fin_r(i)));%aplicamos filtro al hilbert
de la señal,para que luego la envolvente se corresponda con la de la señal
filtrada
hilbert1=hilbert1(ini_analisis(i):fin_r(i));
filtro_h(ini_analisis(i):fin_r(i))= filter(b,a,hilbert1);



%********* Detección de la Frecuencia de la señal de nuevo , Fp y Fs *******%
m=max(z1af1)
p=find(z1af1==m) %En el punto donde capta el pico en la transformada se
encuentra su frecuencia

frec_senyal=frec(p);
%por si coge el valor máximo(correspondiente a la frecuencia) en la parte
%imaginaria, quitarle el valor negativo:
    if frec_senyal<0
    frec_senyal=-frec_senyal
    else
   frec_senyal=frec_senyal
    end

   % else
   % end
fp_min=frec_senyal-2500%fpass minimo con 2.5KHz de margen desde la frecuencia
propia
fp_max=frec_senyal+2500%fpass maximo 2.5KHz de margen desde la frecuencia
propia
fs_min=fp_min-10000%fstop minimo con 10KHz  de margen desde la frecuencia
propia
fs_max=fp_max+10000%fstop maximo con 10KHz de margen desde la frecuencia
propia



%---------- Rango de Banda de paso de margen  5KHz  con frec
central=frecuencia de la señal  ------%

Wp = [fp_min fp_max]/fs;%Frecuencias que deseas pasar
Ws = [fs_min fs_max]/fs;%Tolerancia que ofreces a la horquilla de frecuencias
Rp = 1; Rs = 10;%Tolerancias de la banda de rizado
[n,Wn] = buttord(2*Wp,2*Ws,Rp,Rs)%Definicion
[b,a] = butter(n,Wn);
figure,freqz(b,a,bits,fs)%Parametros y ordenes del filtro + numero de puntos
+ Frecuencia de muestreo
```

```
title(['Butterworth Bandpass Filter  '  num2str(fp_min) 'Hz - '
num2str(fp_max) 'Hz' ])

y(ini_analisis(i):fin_r(i))= filter(b,a,zaf1(ini_analisis(i):fin_r(i)));
ondafiltrada = fftshift(fft(y(ini_analisis(i):fin_r(i))));

figure
subplot(1,2,1),plot(frec,ondafiltrada),title(['ondafiltrada' num2str(i)
'(frecuencia):  '  num2str(fp_min) 'Hz - ' num2str(fp_max) 'Hz' ]);
subplot(1,2,2),plot(t,y(ini_analisis(i):fin_r(i))),title(['ondafiltrada'
num2str(i) '(tiempo):  '  num2str(fp_min) 'Hz - ' num2str(fp_max) 'Hz' ]);

figure,subplot(2,2,2),plot(t,za(ini_analisis(i):fin_r(i))),title(['Señal'
num2str(i) '-Sensor' num2str(s) '- : Onda en tiempo'])
subplot(2,2,1),plot(frec,z1a),title(['Señal' num2str(i) '-Sensor' num2str(s)
'- : Onda en frecuencia(transformada)'])
subplot(2,2,3),plot(frec,ondafiltrada),title(['ondafiltrada' num2str(i)
'(frecuencia):  '  num2str(fp_min) 'Hz - ' num2str(fp_max) 'Hz' ]);
subplot(2,2,4),plot(t,y(ini_analisis(i):fin_r(i))),title(['ondafiltrada'
num2str(i) '(tiempo):  '  num2str(fp_min) 'Hz - ' num2str(fp_max) 'Hz' ]);

figure
set(gca,'fonts',8)
plot(frec,z1a,frec,z1af1,frec,ondafiltrada),title(['SENSOR' num2str(j)
'OndaFiltrada' num2str(i) '(frecuencia)  Paso Banda a Frec.Central:  '
num2str(frec_senyal) 'Hz - '])
legend('S. Original' ,'S. F.P.B 40-60KHz','S. F.P.B Margen 5KHz')


figure
set(gca,'fonts',8)
plot(t,za(ini_analisis(i):fin_r(i)),t,zaf1(ini_analisis(i):fin_r(i)),t,y(ini_
analisis(i):fin_r(i))),title(['SENSOR' num2str(s)  'OndaFiltrada' num2str(i)
'(tiempo)  Paso Banda a Frec.Central:  ' num2str(frec_senyal) 'Hz - '])
legend('S. Original' ,'S. F.P.B 40-60KHz','S. F.P.B Margen 5KHz')




pause

% ---------------  Método 'HILBERT TRANSFORM' ----------%

% ---- Aplicamos filtro Banda Paso 5KHz a la hilbert senyal filtrada -----%
  % --- entre 40-60KHz para obtener la envolvente de la senyal filtrada  ----
%

filtro_h= filter(b,a,filtro_h(ini_analisis(i):fin_r(i)));
envelopeH_filtrado(ini_analisis(i):fin_r(i))=abs(filtro_h);


fase=unwrap(angle(filtro_h)); %fase
fx=diff(unwrap(angle(filtro_h)))./diff(t)/(2*pi); %frecuencia
```

```
%------------------ amplitud  ------------ %

figure,subplot(3,1,1),plot(t,y(ini_analisis(i):fin_r(i)),t,envelopeH_filtrado
(ini_analisis(i):fin_r(i)),'r:'),title(['SENSOR' num2str(s) ':Muestras y
Envolvente(Mediante HILBERT)de la Señal recibida ' num2str(i) ' en el tiempo
parte estable']);
xlabel('t(segundos)');
ylabel('x(t) normalizado')
grid on

%------------------ fase  ------------ %
subplot(3,1,2),plot(t,fase),title(['SENSOR' num2str(s) ':Fase de la Señal
recibida ' num2str(i) ' en el tiempo']);
xlabel('t(segundos)');
ylabel('fase (t)')
grid on
%s=[z1 z];
%s=[z za];%Aqui quedan guardadas todas las señales su número de muestras
correspondiente

%------------------ frecuencia  ------------ %
subplot(3,1,3),plot(t(2:end),fx),title(['SENSOR' num2str(s) ':Frecuencia de
la Señal recibida ' num2str(i) ' en el tiempo']);
xlabel('t(segundos)');
ylabel('frecuencia (t)')
grid on
% --------------------  Cálculo del tiempo de subida --------------------%

% Calculamos de nuevo la amplitud, en la señal Filtrada, en la parte central
% de la senyal, ya que, es normalmente, donde tiene un nivel de amplitud
% mas estable


rango_estable=envelopeH_filtrado(ini_analisis(i)+300:fin_r(i)-250);
amplitud(i)=mean(rango_estable)

% ----------------------

y1(ini_analisis(i):fin_r(i))=envelopeH_filtrado(ini_analisis(i):fin_r(i));


a2=amplitud(i)*0.25;
i2=find(y1>=a2);
i2(i)=min(i2);

format long
Ts_25(i)=i2(i)*ts


y1=0;
%---------------------------
% --------------------  Cálculo del tiempo de bajada --------------------%
```

```
ini_Tb=ini_analisis(i)+350;
fin_Tb=fin_r(i);%-50?
%asi nos hemos desplazado a la parte final para el cálculo del Tb
y2=envelopeH_filtrado(ini_Tb:fin_Tb);% se tiene que tener en cuenta que el
1°valor de y2 realmente corresponde a la muestra ini_Tb,para el posterior
cálcuo del tiempo

a3=amplitud(i)*0.75;
f3=find(y2<=a3);
f3(i)=min(f3)+ini_Tb;

format long
Tb_75(i)=f3(i)*ts

duracion_muestras25_75(i)=-f2(i)+f4(i);
duracion_tiempo25_75(i)=(duracion_muestras25_75(i)).*ts;


y2=0;
 pause
end



% ------------------------------ RECEPCIONES 16,17 ------------------------
%

%ini_r(15)=ini(15)+2400000;% nos desplazamos 2400000=9.65 segundos después,
al último grupo de señales recibidas
%fin_r(15)=fin(15)+2400000;
ini_r(15)=7300000;
fin_r(15)=7251800;

for i=16:1:17

   % -------------------  Deteccion de cada senyal ----------------   %
    if i>=2

    cont2=1;
    cont3=1;

ini(i)=ini_r(i-1)+150000;
fin(i)=fin_r(i-1)+220000;

for j=ini(i):1:fin(i)                                                    %for
desde inicio hasta un margen asegurado de la recepción de la 1
señal:300000*Ts=1.2segundos
 if x(j)>I
     num_muestrasI(cont2)=j;
     cont2=cont2+1;%asi conocemos en qué muestra esta el inicio de la 1
recepción
```

```
                                                % dejamos un margen desde el
inicio para asegurar que campte la amplitud correspondiente a la finalizacion
de la señal
 end
end
ini_r(i)=num_muestrasI(1);%asi coge la primera muestra que ha captado >= que
I
  ini_fin=ini_r(i)+500;

 for k=ini_fin:1:fin(i)
     if x(k)<=F & x(k)>0 %La condición de x(i)>0 , ya que, sino cogia números
negativos de la señal x
         num_muestrasF(cont3)=k;
         cont3=cont3+1;
     end
 end

 fin_r(i)=num_muestrasF(1);%asi coge la primera muestra que ha captado <= que
F
    else

    cont2=1;
    cont3=1;

     for j=1:1:fin1
        %for desde inicio hasta un margen asegurado de la recepción de la 1
señal:300000*Ts=1.2segundos
 if x(j)>I
     num_muestrasI(cont2)=j;
     cont2=cont2+1;%asi conocemos en qué muestra esta el inicio de la 1
recepción                                       % dejamos un margen desde el
inicio para asegurar que campte la amplitud correspondiente a la finalizacion
de la señal
 end
end
ini_r(i)=num_muestrasI(1);%asi coge la primera muestra que ha captado >= que
I
  ini_fin=ini_r(i)+500;


 for k=ini_fin:1:fin1
     if x(k)<=F & x(k)>0 %La condición de x(i)>0 , ya que, sino cogia números
negativos de la señal x
         num_muestrasF(cont3)=k;
         cont3=cont3+1;
     end
 end

 fin_r(i)=num_muestrasF(1);%asi coge la primera muestra que ha captado <= que
F


    end

     %-------------- Calculo de la amplitud propia de la señal ------------%
```

```
 for l=(ini_r(i)-100):1:fin_r(i)
 %muestras de ini y fin de r1

   z(l)=envelopeH(l);

 end

 ts=1/fs;

rango_estable=envelopeH(ini_r(i)+100:fin_r(i)-100);
 amplitud(i)=mean(rango_estable);

I=amplitud(i)*0.25;                                                    %
inicio (muestras) señal 1° recepción
F=amplitud(i)*0.3;

for p=1:1:fin1                                                      %for desde
inicio hasta un margen asegurado de la recepción de la 1
señal:300000*Ts=1.2segundos
 if x(p)>=I
     num_muestrasI(cont1)=p;
     cont1=cont+1;%asi conocemos en qué muestra esta el inicio de la 1
recepción
                                            % dejamos un margen desde el
inicio para asegurar que campte la amplitud correspondiente a la finalizacion
de la señal
 end
end
ini_r(i)=num_muestrasI(1);%asi coge la primera muestra que ha captado >= que
I
  ini_fin=ini_r(i)+500;

 for q=ini_fin:1:fin1
     if x(q)<=F & x(q)>0 %La condición de x(i)>0 , ya que, sino cogia números
negativos de la señal x
         num_muestrasF(cont)=q;
         cont=cont+1;
     end
 end

 fin_r(i)=num_muestrasF(1);%asi coge la primera muestra que ha captado <= que
F

                                             %creamos el nuevo vector para
que posteriormente guarde la señal recibida 1ª entre los margenes del eje
horizontal correctos
 ini_analisis(i)=ini_r(1);
 ini_analisis(i)=ini_r(i)-100;
 fin_r(i)=fin_r(i)+150;
 %z=x(ini_r1:1:fin_r1);
for l=ini_analisis(i):1:fin_r(i)
```

```
    za(l)=x(l);
   hilbert1(l)=hilbert(l);
    envelopeH1(l)=envelopeH(l);
end


%************************************************************%
%****** Filtrado Paso-Banda ***************%
%************************************************************%


%******** Transformada de Fourier de la señal  ************%

t=[ini_analisis(i):1:fin_r(i)].*ts; %rango temporal de la señal
f=1./(t.*ts);%rango frecuencial de la señal

N=length(za(ini_analisis(i):fin_r(i)));%longitud de la señal
frec =[(-1/ts)/2:(1/ts)/(N-1):((1/ts)/2)];%rango frecuencial de la
tranformada

z1a= fftshift(fft(za(ini_analisis(i):fin_r(i))));
figure,subplot(1,2,2),plot(t,za(ini_analisis(i):fin_r(i))),title(['Señal'
num2str(i) '-Sensor' num2str(s) '- : Onda en tiempo'])
subplot(1,2,1),plot(frec,z1a),title(['Señal' num2str(i) '-Sensor' num2str(s)
'- : Onda en frecuencia(transformada)'])

%********* Detección de la Frecuencia de la señal, Fp y Fs *******%

m=max(z1a)
p=find(z1a==m) %En el punto donde capta el pico en la transformada se
encuentra su frecuencia

frec_senyal=frec(p);
%por si coge el valor máximo(correspondiente a la frecuencia) en la parte
%imaginaria, quitarle el valor negativo:
if frec_senyal<0
    frec_senyal=-frec_senyal
else
   frec_senyal=frec_senyal
end




%-------- Aplicamos Filtro Paso Banda de 35 a 65 KHz a una frecuencia de unos
60KHz ---- %



  fp_min=40000;%fpass minimo
fp_max=60000;%fpass maximo
```

```
fs_min=35000;%fstop minimo con 2.5KHz  de margen
fs_max=65000;%fstop maximo con 2.5KHz de margen


Wp = [fp_min fp_max]/fs;%Frecuencias que deseas pasar
Ws = [fs_min fs_max]/fs;%Tolerancia que ofreces a la horquilla de frecuencias
Rp = 1; Rs = 10;%Tolerancias de la banda de rizado
[n,Wn] = buttord(2*Wp,2*Ws,Rp,Rs)%Definicion
[b,a] = butter(n,Wn);
figure,freqz(b,a,bits,fs)%Parametros y ordenes del filtro + numero de puntos
+ Frecuencia de muestreo
title(['Butterworth Bandpass Filter  '  num2str(fp_min) 'Hz - '
num2str(fp_max) 'Hz' ])

    zaf1(ini_analisis(i):fin_r(i))=
filter(b,a,za(ini_analisis(i):fin_r(i)));%aplicamos filtro a la señal
z1af1= fftshift(fft(zaf1(ini_analisis(i):fin_r(i))));

figure,subplot(1,2,1),plot(frec,z1af1),title(['ondafiltrada' num2str(i)
'F.Paso Banda (frecuencia):  '  num2str((fp_min)) 'Hz - ' num2str(fp_max)
'Hz' ]);
subplot(1,2,2),plot(t,zaf1(ini_analisis(i):fin_r(i))),title(['ondafiltrada'
num2str(i) 'F.Paso Banda (tiempo):  '  num2str((fp_max)) 'Hz - '
num2str((fp_max)) 'Hz' ]);

% ---- Aplicamos filtro Banda Paso entre 40-60KHz a la hilbert senyal -----%
  % --- para obtener la envolvente de la senyal filtrada  ----  %

  %hilbert1(ini_analisis(i):fin_r(i))=
filter(b,1,hilbert1(ini_analisis(i):fin_r(i)));%aplicamos filtro al hilbert
de la señal,para que luego la envolvente se corresponda con la de la señal
filtrada
hilbert1=hilbert1(ini_analisis(i):fin_r(i));
filtro_h(ini_analisis(i):fin_r(i))= filter(b,a,hilbert1);



%********* Detección de la Frecuencia de la señal de nuevo , Fp y Fs *******%
m=max(z1af1)
p=find(z1af1==m) %En el punto donde capta el pico en la transformada se
encuentra su frecuencia

frec_senyal=frec(p);
%por si coge el valor máximo(correspondiente a la frecuencia) en la parte
%imaginaria, quitarle el valor negativo:
    if frec_senyal<0
    frec_senyal=-frec_senyal
    else
   frec_senyal=frec_senyal
    end

   % else
   % end
fp_min=frec_senyal-2500%fpass minimo con 2.5KHz de margen desde la frecuencia
propia
```

```
fp_max=frec_senyal+2500%fpass maximo 2.5KHz de margen desde la frecuencia
propia
fs_min=fp_min-10000%fstop minimo con 10KHz  de margen desde la frecuencia
propia
fs_max=fp_max+10000%fstop maximo con 10KHz de margen desde la frecuencia
propia


%---------- Rango de Banda de paso de margen  5KHz  con frec
central=frecuencia de la señal  ------%

Wp = [fp_min fp_max]/fs;%Frecuencias que deseas pasar
Ws = [fs_min fs_max]/fs;%Tolerancia que ofreces a la horquilla de frecuencias
Rp = 1; Rs = 10;%Tolerancias de la banda de rizado
[n,Wn] = buttord(2*Wp,2*Ws,Rp,Rs)%Definicion
[b,a] = butter(n,Wn);
figure,freqz(b,a,bits,fs)%Parametros y ordenes del filtro + numero de puntos
+ Frecuencia de muestreo
title(['Butterworth Bandpass Filter  '  num2str(fp_min) 'Hz - '
num2str(fp_max) 'Hz' ])

y(ini_analisis(i):fin_r(i))= filter(b,a,zaf1(ini_analisis(i):fin_r(i)));
ondafiltrada = fftshift(fft(y(ini_analisis(i):fin_r(i))));

figure
subplot(1,2,1),plot(frec,ondafiltrada),title(['ondafiltrada' num2str(i)
'(frecuencia):  '  num2str(fp_min) 'Hz - ' num2str(fp_max) 'Hz' ]);
subplot(1,2,2),plot(t,y(ini_analisis(i):fin_r(i))),title(['ondafiltrada'
num2str(i) '(tiempo):  '  num2str(fp_min) 'Hz - ' num2str(fp_max) 'Hz' ]);

figure,subplot(2,2,2),plot(t,za(ini_analisis(i):fin_r(i))),title(['Señal'
num2str(i) '-Sensor' num2str(s) '- : Onda en tiempo'])
subplot(2,2,1),plot(frec,z1a),title(['Señal' num2str(i) '-Sensor' num2str(s)
'- : Onda en frecuencia(transformada)'])
subplot(2,2,3),plot(frec,ondafiltrada),title(['ondafiltrada' num2str(i)
'(frecuencia):  '  num2str(fp_min) 'Hz - ' num2str(fp_max) 'Hz' ]);
subplot(2,2,4),plot(t,y(ini_analisis(i):fin_r(i))),title(['ondafiltrada'
num2str(i) '(tiempo):  '  num2str(fp_min) 'Hz - ' num2str(fp_max) 'Hz' ]);

figure
set(gca,'fonts',8)
plot(frec,z1a,frec,z1af1,frec,ondafiltrada),title(['SENSOR' num2str(j)
'OndaFiltrada' num2str(i) '(frecuencia)  Paso Banda a Frec.Central:  '
num2str(frec_senyal) 'Hz - '])
legend('S. Original' ,'S. F.P.B 40-60KHz','S. F.P.B Margen 5KHz')

figure
set(gca,'fonts',8)
plot(t,za(ini_analisis(i):fin_r(i)),t,zaf1(ini_analisis(i):fin_r(i)),t,y(ini_
analisis(i):fin_r(i))),title(['SENSOR' num2str(s)  'OndaFiltrada' num2str(i)
'(tiempo)  Paso Banda a Frec.Central:  ' num2str(frec_senyal) 'Hz - '])
legend('S. Original' ,'S. F.P.B 40-60KHz','S. F.P.B Margen 5KHz')
```

```
pause

% ---------------  Método 'HILBERT TRANSFORM' ----------%

% ---- Aplicamos filtro Banda Paso 5KHz a la hilbert senyal filtrada -----%
  % --- entre 40-60KHz para obtener la envolvente de la senyal filtrada  ----
%

filtro_h= filter(b,a,filtro_h(ini_analisis(i):fin_r(i)));
envelopeH_filtrado(ini_analisis(i):fin_r(i))=abs(filtro_h);


fase=unwrap(angle(filtro_h)); %fase
fx=diff(unwrap(angle(filtro_h)))./diff(t)/(2*pi); %frecuencia



%------------------ amplitud  ------------ %

figure,subplot(3,1,1),plot(t,y(ini_analisis(i):fin_r(i)),t,envelopeH_filtrado
(ini_analisis(i):fin_r(i)),'r:'),title(['SENSOR' num2str(s) ':Muestras y
Envolvente(Mediante HILBERT)de la Señal recibida ' num2str(i) ' en el tiempo
parte estable']);
xlabel('t(segundos)');
ylabel('x(t) normalizado')
grid on

%------------------ fase  ------------ %
subplot(3,1,2),plot(t,fase),title(['SENSOR' num2str(s) ':Fase de la Señal
recibida ' num2str(i) ' en el tiempo']);
xlabel('t(segundos)');
ylabel('fase (t)')
grid on
%s=[z1 z];
%s=[z za];%Aqui quedan guardadas todas las señales su número de muestras
correspondiente

%------------------ frecuencia  ------------ %
subplot(3,1,3),plot(t(2:end),fx),title(['SENSOR' num2str(s) ':Frecuencia de
la Señal recibida ' num2str(i) ' en el tiempo']);
xlabel('t(segundos)');
ylabel('frecuencia (t)')
grid on
% --------------------  Cálculo del tiempo de subida --------------------%

% Calculamos de nuevo la amplitud, en la señal Filtrada, en la parte central
% de la senyal, ya que, es normalmente, donde tiene un nivel de amplitud
% mas estable


rango_estable=envelopeH_filtrado(ini_analisis(i)+300:fin_r(i)-250);
amplitud(i)=mean(rango_estable)
```

```
% ----------------------

y1(ini_analisis(i):fin_r(i))=envelopeH_filtrado(ini_analisis(i):fin_r(i));

a2=amplitud(i)*0.25;
i2=find(y1>=a2);
i2(i)=min(i2);

format long

Ts_25(i)=i2(i)*ts
y1=0;
%----------------------------
% --------------------  Cálculo del tiempo de bajada --------------------%

ini_Tb=ini_analisis(i)+350;
fin_Tb=fin_r(i);%-50?
%asi nos hemos desplazado a la parte final para el cálculo del Tb
y2=envelopeH_filtrado(ini_Tb:fin_Tb);% se tiene que tener en cuenta que el
1°valor de y2 realmente corresponde a la muestra ini_Tb,para el posterior
cálcuo del tiempo

a2=amplitud(i)*0.75;
f2=find(y2<=a2);
f2(i)=min(f2)+ini_Tb;%sumamos ini_Tb ya que la 1 casilla de y2(valor del
tiempo) corresponde a la casilla ini_Tb

format long
Tb_50(i)=f2(i)*ts%el número de casilla(valor tiempo normalizado)*ts= valor
del tiempo(desnormalizado) que corresponde al alcance del % de amplitud
durante el tiempo de bajada

duracion_muestras25_75(i)=-f2(i)+f4(i);
duracion_tiempo25_75(i)=(duracion_muestras25_75(i)).*ts;



y2=0;
 pause
end
```

Appendix 2. Acoustic Array Calibration and Signal Processing for UHE Neutrinos Generation.

Acoustic Array Calibration and Signal Processing for UHE Neutrinos Generation

W.Ooppakaew, S.Danaher
School of CEIS
Northumbria University
Newcastle, UK
wichian.ooppakaew@unn.ac.uk
sean.danaher@unn.ac.uk

M.Saldaña
IGIC
Universidad Politécnica de Valencia
Valencia, Spain
masalcos@epsg.upv.es

Abstract— **The calibration and design of an eight-hydrophone linear array has been developed for the generation of emulated Ultra High Energy (UHE) neutrino-induced pulses. The acoustic array simulates the acoustic pulse created from a neutrino interaction in water by generating a coherently emitted acoustic bipolar pulse. The calibrator is developed using signal processing methods using experimental measurements to characterise the hydrophone system. An 8 channel PIC hydrophone array module has been built for processing and control. A linear array simulation for the neutrino pulses production has been studied in order to predict the directivity and shape of the acoustic bipolar pulse at the ANTARES neutrino detector.**

Keywords: Array hydrophone calibration; UHE neutrinos; Acoustic detection; PIC module; array simulation.

INTRODUCTION

In order to evaluate the actual behaviour of acoustic neutrino detector in the field, acoustic transmitters are needed to send artificial acoustic signatures from UHE neutrino interactions in the sea. The transmitters have to be able to imitate the UHE neutrino acoustic pulse, in directivity (pancake) and shape (a short bipolar pulse). Furthermore the detector site is located at a depth of 2475 m underwater. Due these limitations, it is not an easy task to design a system able to reproduce an acoustic bipolar pulse with such characteristics. The deployment and operation in site have to be considered in terms on the system design as well. The use of a linear array of omni-directional transmitters has been studied and developed to achieve the proposed objective.

AIM

This research utilizes an eight-hydrophone calibrated array for the generation of Ultra High Energy neutrino-induced pulses at the frequency of 23 kHz. Signal processing techniques are applied to array hydrophone modeling and experimental data generated in a laboratory water tank are used and compared to the calibration system. Using such an array has the advantage that would allow precise calibration of existing and planned acoustic neutrino telescope.

An acoustic generation module of 8 channels has been built using PIC microcontrollers for process and control [1]; it will be used to improve the speed and precision of data transmission in underwater communication using the precise control of the amplitude and phase of the signal.

DEEP-SEA ACOUSTIC NEUTRINO DETECTION

The ANTARES module for Acoustic Detection under the sea (AMADEUS)

The ANTARES (Astronomy with a Neutrino Telescope and Abyss environmental RESearch) Collaboration [2] built a large effective area water Cherenkov detector in the deep Mediterranean Sea optimised for the detection of muons from high-energy astrophysical neutrinos. A large amount of

sensors of different kinds had to be deployed and connected in deep sea to become a network of coordinated underwater sensors looking for neutrinos and monitoring the deep sea.

The AMADEUS project [3] was conceived to perform a feasibility study for a potential future large scale acoustic neutrino detector. For this purpose, a dedicated array of acoustic sensors was integrated into the ANTARES neutrino telescope.

The Thermo-Acoustic model

Measuring acoustic pressure pulses in huge underwater acoustic arrays is a promising approach for the detection of cosmic neutrino with energies exceeding 100 PeV. The particle cascades that evolve when neutrinos interact with nuclei in water produce pressure signals. The resulting energy deposition in a cylindrical volume of a few centimetres in radius and several metres in length (from 5m to 10 m) lead a local heating of the medium, which is near instantaneous with respect to the acoustic process. This temperature change induces an expansion or contraction of the medium depending on its volume expansion coefficient.

According to the thermo acoustic model, the accelerated motion of the heated volume—a micro-explosion—forms a pressure pulse of bipolar shape, which propagates in the surrounding medium. The wave equation describing the pulse is:

$$\vec{\nabla}^2 p(\vec{r},t) - \frac{1}{c_s^2}\cdot\frac{\partial^2 p(\vec{r},t)}{\partial t^2} = -\frac{\alpha}{C_p}\cdot\frac{\partial^2 \varepsilon(\vec{r},t)}{\partial t^2} \quad (1)$$

Hear $p(\vec{r},t)$ denotes the pressure at a given place and time, c_s the speed of sound in the medium, C_p its specific heat capacity, α the thermal expansion coefficient and $\varepsilon(\vec{r},t)$ the energy deposition density of the particles.

The spatial and temporal distribution of ε is not accessible to laboratory experiments at the relevant primary neutrino energies $E \approx 10^{18}\ eV$ [4,5] and hence is subject to uncertainties. Simulations depend on both the extrapolation of parameterisations for lower energies into this regime and on the transcription of simulations for extended air showers to showers in water. Monte Carlo simulation of neutrino interactions in water for a cascade energy has been developed in previous studies [6,7], where is demostrated if the energy deposition is modelled using Monte Carlo points with a density proportional to energy, the pressure will be a scaled derivative histogram of the flight times to the observer.

Attenuation in seawater

The acoustic attenuation in seawater is almost totally caused by absorption. In the 1-100 kHz region it is dominated by a chemical relaxation process that is connected with the association-dissociation of magnesium sulphate ($MgSO_4$) ions under the pressure of the sound wave. Below 1 kHz a similar mechanism involving boric acid ($(B(OH)_3$) is responsible for much of the observed attenuation.

Taken together these mechanisms result in an attenuation of acoustic waves in seawater and a velocity of sound, which are both frequency dependent. Experimentally however whereas it is straightforward to estimate the magnitude of $|a|$ of the complex attenuation it is very difficult to determine the phase angle of a and no current measurements exist in the literature. The magnitude of the attenuation however is well

measured and the definitive work in this area is considered to be that of Francois and Garrison [8]. More recently, Ainslie and McColm [9] have published a simplified parameterization of the magnitude of the attenuation in seawater, which maintains a similar accuracy to the parameterizations of Francois and Garrison. This is a function not only of frequency but also depends on depth, *z*, salinity, S, temperature, T and pH. Whereas there are no direct measurements of the attenuation angle, Lieberman [10] gives a clear presentation of the chemical processes causing the attenuation while Niess and Bertin [11] have published a complex attenuation formula based on Mediterranean conditions. The ACORNE attenuation method [6] presents a complex version of the Ainslie and McColm formulation, which retains the attenuation magnitude but introduces the phase shifts predicted by Lieberman. In essence the attenuation consists of three components, two of these are complex, high pass filters with cut off frequencies ω_B (~$2\pi \times 10^3$ rad s^{-1}) for boric acid and ω_{Mg} (~$2\pi \times 10^5$ rad s^{-1}) for magnesium sulphate. The third is the pure water component, which is real. The ACORNE parameterization uses a_x values that are the respective attenuation coefficients in dB/km; boric acid (w_B), magnesium sulphate (w_{Mg}), boric acid and magnesium sulphate attenuation coefficients (a_B, a_{Mg}), water coefficient attenuation (a_w), and total attenuation coefficient ($a_{dB/km}$):

$$w_B = 1560\pi\sqrt{\frac{S}{35}}e^{T/26} \quad w_{Mg} = 84000\pi e^{T/17}, a_B = \frac{1.893\times10^{-4}}{2\pi}e^{\frac{pH-8}{0.56}}$$

$$a_{Mg} = \frac{0.52\times10^{-3}}{2\pi}(1+\frac{T}{43})\frac{S}{35}e^{\frac{-z}{6}}, \; a_w = \frac{49\times10^{-9}}{4\pi^2}e^{-(T/27+z/17)}$$

$$a_{dB/km} = \frac{a_B w_B s}{s+w_B} + \frac{a_{Mg} w_{Mg} s}{s+w_{Mg}} + a_w w^2 \quad \text{where } s = i\omega \qquad (2)$$

For the Mediterranean sea the conditions are: *T* = 15ºC; *S* = 37; pH = 7:9; *z* = 2km. This new method of computing the acoustic signal complex attenuation for neutrino shower in water and ice has been described in collaboration with the ACORNE [6]. The method allows the most up to date knowledge of the attenuation to be incorporated naturally, which is known to be complex in nature.

METHODOLOGY

The array calibration development can be classified in three phases. In the first phase, signal processing and measurements in water tank are used for the single hydrophone calibration. The characterisation system of the hydrophones is designed to generate the sought bipolar pulse. In a second phase, the eight transmitters are individually checked and validated for the calibration done. Then, the complete eight hydrophone array is placed in the water tank test with the purpose of studying the bipolar signal amplitude transmitted as function of the tension in the transducer, using both the eight channel PIC module and a commercial module for comparison. In a third phase, the eight hydrophones array is simulated by signal processing where is introduced the real array design side, and the environment conditions (Mediterranean sea attenuation, receiver distance), with the objective of predicting the pattern directivity and shape of the bipolar pulse at the detector, determining the correct 8 hydrophone's array length which could send the signal with the 1º 'pancake' directivity.

Signal processing techniques for single hydrophone calibration

Linear Time Invariant (LTI) signal processing can successfully be used to calibrate hydrophones and that standard signal processing techniques can be used to produce arbitrary acoustic waveforms.

The LTI model for a transmit hydrophone consists of three parts: an RC electrical circuit coupled to a set of damped mechanical masses and an impedance matching network to couple the hydrophone to the water. This can be represented either in State Space or as a transfer function; it is described in previous publication [1]. The block diagram of signal processing techniques for calibration is shown in Fig. 1.

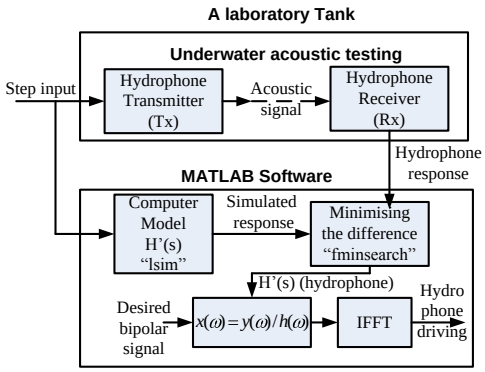

Figure 1. Block diagram of the signal processing techniques used for calibration.

Experimental environment and measures

The calibration system is implemented in a rectangular glass water test tank of 1.52 m in length, 0.60 m in width and 0.60 m in depth. The eight hydrophones under calibration are identical robust spherical reference hydrophones (RESON TC 4033) used as transducers to transmit the desired acoustic signals. The RESON TC 4033 provides uniform omni-directional characteristics within the full useable frequency range of 1 Hz to 140 kHz. It has a factory-calibrated transmitting sensitivity of 120 dB ref 1µPa/V@ 1m at 23 kHz.

Matlab computer software is used to create an ideal step signal which is injected to LabVIEW (NI-USB 6211) software, which has a 16 bit analogue-to-digital converter (ADC) sampled at 250 kHz. It is then amplified using a PA94 power amplifier chip (gain of 17) and it's sent out to a single transmitter hydrophone in underwater. The output signal is detected by a wide range bandwidth hydrophone (a Bruel & Kjaer type 8106), general-purpose transducer for making absolute sound measurements over the frequency range from 7 Hz to 80 KHz with receiving sensitivity of -173dB ref 1V/µPa. It provides a flat frequency response and omni-directional characteristics over wide range. The output data from the receiver is the hydrophone step response which is recorded for a data acquisition module (Tektronik TDS 2002 B); it is shown in Fig. 2.

The know input to the hydrophone, it means the step signal, is injected into the LTI software model and the outputs the real and model hydrophones are matched by reducing the sum squared error (Fig. 2). The order of the LTI model is gradually increased to ensure sufficient goodness on fit. A fifth-order scaled transfer function (TF) is fitted to this step response (Eq. (3)). The TF is a mathematical representation of the relationship between the input and output of a LTI system.

The input driving signal for 23 kHz bipolar pulse is resulted from replacing fitted transfer function and the desired bipolar signal at 23 kHz. An inverse Fourier transform is then used to convert the input driving signal from the frequency to time domain (Fig. 3). This is the driving pulse used as input in the hydrophone transmitter (using the Transfer Function obtained Eq.(3)) to send the 23 kHz bipolar pulse.

Step response fitting of transmitter hydrophone

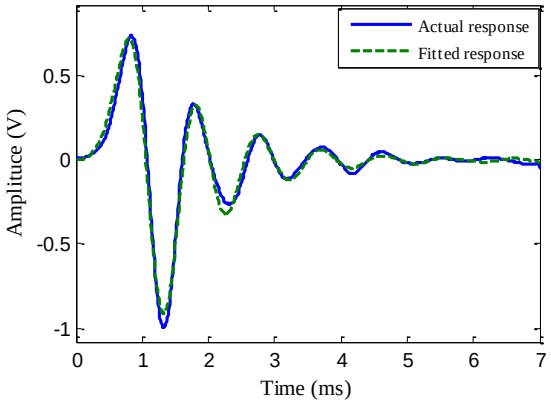

Figure 2. Fitting the step response simulated with the measured for the hydrophone transfer function.

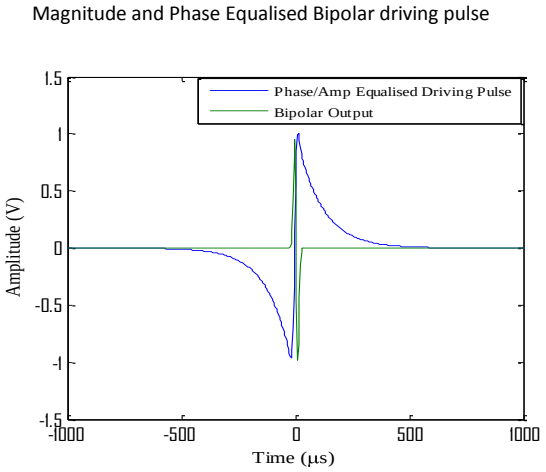

Figure 3. Input driving pulse and output 23 KHz bipolar pulse simulated.

The transfer function $H(s)$ obtained is:

$$\frac{2.436\,s^2 - 0.1226\,s - 0.08506}{0.002913\,s^5 + 0.01982\,s^4 + 0.5279\,s^3 + 2.434\,s^2 + 18.65\,s + 45.9} \quad (3)$$

The desired excitation signal obtained from Matlab to achieve the 23 kHz bipolar pulse is transferred to flash program memory of PIC via serial port protocol. The data is permanently kept in flash program memory until it is replaced by new data. The PIC system is now stand alone and when it receives a trigger pulse outputs this 16 bit digital data to the DAC at a sampling rate of 500 kHz. The signal is amplified by PA94 hydrophone power amplifier chip and sent out to transmitter hydrophone in underwater. The acoustic signal is detected by the acoustic receiver hydrophone and pre-amplified. The data is kept by the Data acquisition module. The block diagram of the calibration system is shown:

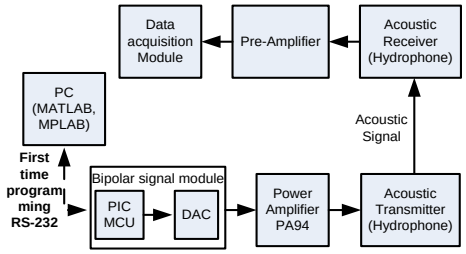

Figure 4. Bipolar signal module for the single hydrophone system calibration.

The experimental data shows successful hydrophone calibration results for the 23 kHz bipolar pulse transmission, showing excellent agreement between the simulation and experiment. Moreover, the bipolar pulse generated using the PIC module is compared with the NI PXI-6713 commercial module giving similar results.

Hydrophone Array test results and prediction

The bipolar driving pulse obtaining in the calibration for a single hydrophone is checked in

the water tank test for each hydrophone, showing a 23 kHz bipolar pulse transmitted with same amplitude, shape and duration for the 8 hydrophones under calibration, being validated for the calibration done. The complete 8 array hydrophone has been checked getting 8 times more amplitude than with a single hydrophone. This confirms that the array can send 556.6 Pa at 1 meter, which corresponds to bipolar pulse pressure amplitude of 225.3 mPa at the AMADEUS system without attenuation.

The ACORNE method of computing the natural complex attenuation presents in the seawater [6] is an accurate tool to predict the 23 kHz bipolar pulse amplitude at the AMADEUS system, which is 2475m sdepth. The Fig. 5 shows it for a pressure of 1 Pa:

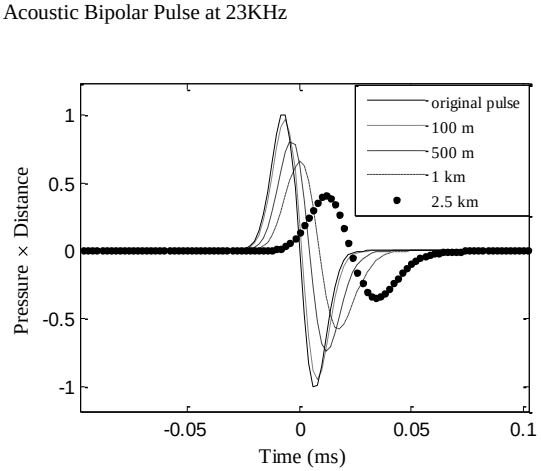

Figure 5. Simulation of the neutrino UHE attenuation with the distance increase in the Mediterranean Sea using ACORNE method

The bipolar pulse amplitude at 23 KHz and 2475m of depth is attenuated 0.5785 Pa per 1 Pa (attenuation of 0.4215 or -7.5dB), moreover the signal has a phase shift, which slightly distorts the pulse. Hence the hydrophone array signal would arrive at the AMADEUS system with about 95 mPa of pressure amplitude with attenuation of the Mediterranean Sea conditions. Taking, the AMADEUS system can detect a signal of 20 mPa at calm sea in the frequency range from 1 to 50 KHz, into consideration, and knowing the environment of the Mediterranean Sea is normally mild, the amplitude pressure of 95 mPa should be adequate to be detected by the AMADEUS system sensors.

ARRAY SIMULATION FOR THE DEPLOYMENT AT ANTARES

Introduction

Computing methods of acoustic signal for neutrino shower simulation and the calculation of the sound signal in water at the detector have been described in previous papers [6, 7]. The program allows to be generated in the medium over a wide range of energy (10^5–10^{12} GeV).

The computing method of ACORNE collaboration [6] which includes the complex attenuation effect in the sea water is assumed to simulate the 8 hydrophone array system. It is used to study the array design and size in order to achieve the best approximation to the UHE neutrino-induced pulses properties in the transmission of the artificial bipolar signal pulse. It is referenced to the bipolar pulse signal shape and directivity at the acoustic receiver sensors belonged to the ANTARES system.

Array simulation modelling

For the simulation, shower parameters as a function of energy are generated, these are stored in a matrix of radial and longitudinal distributions. From the shower parameter matrix a number of points are thrown by a Monte Carlo, the points are generated in polar coordinates. For the array shower the points are split in 8 sphere storey

(number of array hydrophones).The acoustic integrator, which works in Cartesian coordinates, calculates the pressure as a scaled derivative histogram of the flight times to the observer [6,7]. The complex attenuation is assumed in the acoustic integrator.

The neutrino creates a hadronic shower of approximately 10 m in length and 5 cm in radius. For the simulation, the deposited energy is binned in a cylinder of 10 meters in length and 2.5 cm in width which gives approximated characteristics to the bipolar signal created for the neutrino interaction, referred to bipolar pulse shape and directivity. This is used as reference to compare it with the array shower generation, which uses the same side as the cylinder simulation but it is split in 8 spheres with equitable centres along the 10 meters in length. The length is also compared for 8 and 6 meters in order to study the length with the most approximation in shape and 'pancake' angle of neutrinos bipolar pulse.

In the coordinate system is chosen such that the neutrino interacts at the origin and travels vertically along the *z* axis where the value of *z* increases with depth and the origin. The point (0, 0,$-Z_p$) is chosen such that the maximum 'pancake', it is the point at 0°. The values of *Zp* is energy dependent varying from approximately 460cm (10^5 GeV) to 780cm (10^{12} GeV). The radial distribution gets broader with the age (depth) of the shower; the earlier part contributes more to the pulse energy than the later part of the shower. A fit to seawater data yields a relationship to determine *Zp* from the position of the shower centroid (Z_c) or from the primary energy *E* (in GeV):

$$z_p = 1.05 z_c - 0.874 \quad , \quad z_p = -0.046(\log_{10} E)^2 + 1.3\log_{10} E - 0.84 \tag{4}$$

For the analysis the observer is positioned at 2475m from the shower in the centre of the acoustic pancake along the *x* axis, simulating the deployment at the ANTARES detector, the array simulation system for 8 meters length shower is shown in Fig. 6. As the previous publish results have shown [3], the spread of the pancake decreases increasing shower energy. For the simulation, a 10^{11} GeV shower energy deposition is chosen, which was used in previous studies for comparison.

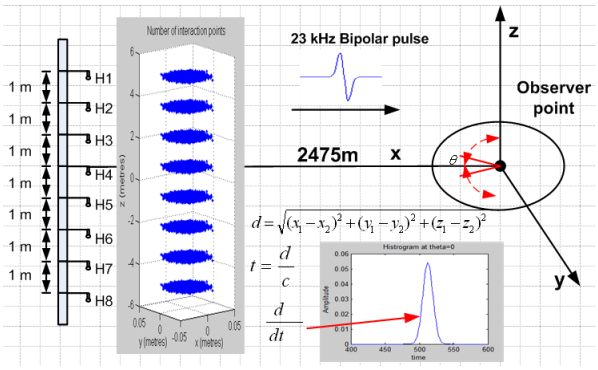

Figure 6. Simulation of the 8 hydrophone array transmission to ANTARES system.

Comparison and results

The array has been analysed with the simulation to know the proper length with what is obtaining the most directive angle maintaining the bipolar pulse shape. An energy equivalent to a 10^{11} GeV shower is shared between eight-spheres for a 6, 8 and 10 meters array length and also a uniform energy distribution along a 10 meter cylinder is shown for comparison. The observer is at 2475m and the result shown in Fig. 7, which gives the pulse energy at the detector vs angular

spread of the pancake between 0˚ and 1˚. The pancake spread decreases with array length. The pressure amplitude of the bipolar signal as a function of time for the eight-sphere array with 8 m from 0˚ to 1˚, again for a 10^{11} GeV energy deposition. The figure shows that bipolar pulse shape as a function of angle for the 8 m eight-sphere array imitate properly the behaviour the UHE neutrino acoustic pulse.

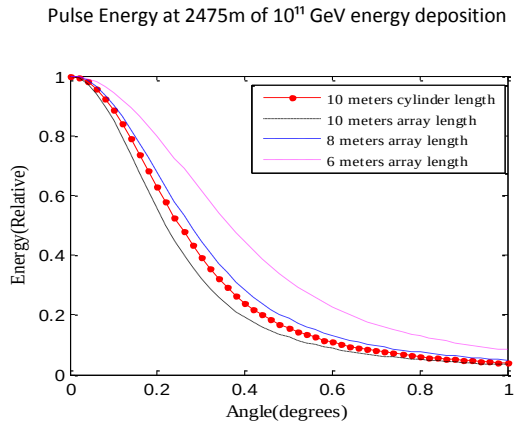

Figure 7. Energy per angle at 2475 meters from 10^{11} GeV of thermal energy shower deposition, under Mediterranean Sea conditions

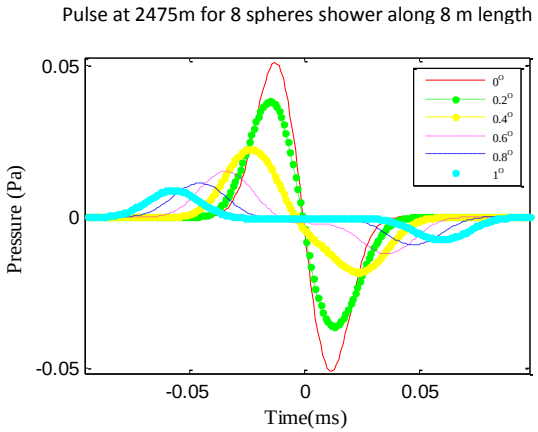

Figure 8. Amplitude (Pa) in time (ms) of the Acoustic bipolar pulse generated from a 10^{11} GeV thermal energy shower deposition at 2475 meters under Mediterranean Sea conditions. The array shower simulation is 8 meters length.

Conclusion

The acoustic hydrophone array calibration has been developed for UHE neutrino detection using the combination and comparison of signal processing techniques and experimental data generation, showing excellent agreement. The linear hydrophone array simulation shows that the eight hydrophones arranged over an eight meters spacing structure can mimic the anticipated pancake behaviour predicted from neutrino-induced showers as well as the acoustic bipolar pulse shape and amplitude at the ANTARES system.

In future work, the array system calibrated is expected to be placed in a structure of 8 meters length according with the simulated results and it will be used at sea sites to send the acoustic bipolar signal for UHE neutrinos detection at the ANTARES system in September of 2011. The 8 channel PIC hydrophone array module built will be used for controlling and processing during the deployment.

Acknowledgment

We would like to thank to the Ministry of Science and Technology, Royal Thai Government who sponsor this work with a full time PhD studentship. Also, we thank to the Erasmus Programme of the European Union who funds part of this project with a 6 month full time internship.

References

[1] W. Ooppakaew,S. Danaher, “Hydrophone Calibration Based on Microcontrollers for Acoustic Detection of UHE Neutrinos” Nucl.Instr. and Meth.A (2011),doi:10.1016/j.nima.2010.11.142

[2] J.A.Aguilar, “ANTARES:The first undersea neutrino telescope” Nucl.Instr. and Meth.A (2011),[arxiv:1104.1607v1] .

[3] J.A.Aguilar, “AMADEUS:The Acoustic neutrino detection system of the ANTARES Deep-Sea neutrino telescope”, Nucl.Instr. and Meth.A (2010),doi:10.1016/j.nima.2010.09.53.

[4] K.Greisen,Phys.Rev.Lett 16(1966)748.

[5] G:T Zatsepin, V.A kuz´min,JETP Lett,4(1906)78;G.T.Zatsepin, V.A.Kuz´min, Z.Eksp.Teor.Fiz(1966)114.

[6] S.Bevan, "Study of the acoustic siganture of UHE neutrino interactions in water and ice" Nucl.Instr. and Meth.A 607 (2009) 398-411.

[7] S. Bevan "Simulation of Ultra High Energy Neutrino Interactions in Ice and Water" et al. / Astroparticle Physics 28 (2007) 366–379

[8] R. E. Francois, G. R. Garrison, "Sound absorption based on ocean measurements: Part I:Pure water and magnesium sulfate contributions," "Sound absorption based on ocean measurements: Part II:Boric acid contribution and equation for total absorption"

[9] M. A. Ainslie and J. G. McColm "A simplified formula for viscous and chemical absorption in seawater" Journal of the Acoustical Society of America 103(3) (1998) 1671-1672.

[10] L. N. Lieberman, "The Origin of Sound Absorption in Water and in Sea Water" The Journal of the Acoustical Society of America 20(6) (1948) 868-873.

[11] V. Niess and V. Bertin, "Underwater Acoustic Detection of Ultra High Energy Neutrinos", Astropart. Phys. 26(4-5) (2006) 243-25